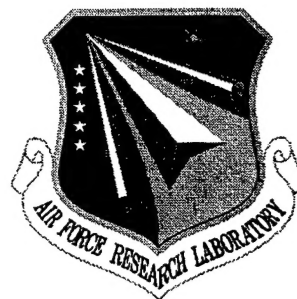AFRL-IF-RS-TR-1998-198
Final Technical Report
October 1998

MATERIALS AND PROCESSES FOR OPTICAL MEMORIES

University of California, Irvine

APPROVED FOR PUBLIC RELEASE; DISTRIBUTION UNLIMITED.

19981210 025

**AIR FORCE RESEARCH LABORATORY
INFORMATION DIRECTORATE
ROME RESEARCH SITE
ROME, NEW YORK**

This report has been reviewed by the Air Force Research Laboratory, Information Directorate, Public Affairs Office (IFOIPA) and is releasable to the National Technical Information Service (NTIS). At NTIS it will be releasable to the general public, including foreign nations.

AFRL-IF-RS-TR-1998-198 has been reviewed and is approved for publication.

APPROVED: ALBERT A. JAMBERDINO
Project Engineer

FOR THE DIRECTOR: JOSEPH CAMERA, Deputy Chief
Information and Intelligence Exploitation Division
Information Directorate

REPORT DOCUMENTATION PAGE

Public reporting burden for this collection of information is estimated to average 1 hour per response, including the time for reviewing instructions, searching existing data sources, gathering and maintaining the data needed, and completing and reviewing the collection of information. Send comments regarding this burden estimate or any other aspect of this collection of information, including suggestions for reducing this burden, to Washington Headquarters Services, Directorate for Information Operations and Reports, 1215 Jefferson Davis Highway, Suite 1204, Arlington, VA 22202-4302, and to the Office of Management and Budget, Paperwork Reduction Project (0704-0188), Washington, DC 20503.

1. AGENCY USE ONLY *(Leave blank)*	2. REPORT DATE	3. REPORT TYPE AND DATES COVERED	
	October 1998	Final	Sep 93 - Jun 98

4. TITLE AND SUBTITLE	5. FUNDING NUMBERS
MATERIALS AND PROCESSES FOR OPTICAL MEMORIES	C - F30602-93-C-0231

6. AUTHOR(S)

Peter M. Rentzepis and Sadik C. Esener

5. FUNDING NUMBERS

C - F30602-93-C-0231
PE - 62702F
PR - 4594
TA - 15
WU - K7

7. PERFORMING ORGANIZATION NAME(S) AND ADDRESS(ES)	8. PERFORMING ORGANIZATION REPORT NUMBER
University of California, Irvine Irvine CA 92597	N/A

9. SPONSORING/MONITORING AGENCY NAME(S) AND ADDRESS(ES)	10. SPONSORING/MONITORING AGENCY REPORT NUMBER
AFRL/IFED 32 Brooks Road Rome NY 13441-4114	AFRL-IF-RS-TR-1998-198

11. SUPPLEMENTARY NOTES

AFRL Project Engineer: Albert A. Jamberdino/IFED/(315) 330-2845

12a. DISTRIBUTION AVAILABILITY STATEMENT	12b. DISTRIBUTION CODE
Approved for public release; distribution unlimited.	

13. ABSTRACT *(Maximum 200 words)*

This project had two major aims:

a. The design and development of new materials which are stable at room temperature to be used as two photon 3D memory materials.

b. Develop system capabilities and spatial light modulators for fast access two Photon memory systems.

Both goals have been achieved and a prototype system encompassing these objectives has been built.

14. SUBJECT TERMS	15. NUMBER OF PAGES
Optical storage, volumetric memory, storage and retrieval, two-photon material, photochromic media	52
	16. PRICE CODE

17. SECURITY CLASSIFICATION OF REPORT	18. SECURITY CLASSIFICATION OF THIS PAGE	19. SECURITY CLASSIFICATION OF ABSTRACT	20. LIMITATION OF ABSTRACT
UNCLASSIFIED	UNCLASSIFIED	UNCLASSIFIED	UL

TABLE OF CONTENTS

LIST OF FIGURES:

LIST OF SCHEMES:

LIST OF TABLES

iii

I.   Goals and Achievements.

This project had two major aims:

a. The design and development of new materials which are stable at room temperature to be used as two photon 3D memory materials.
Develop system capabilities and spatial light modulators for fast access two Photon memory systems.

Both goals have been achieved and a prototype system encompassing these objectives has been built.

The materials and system achievements are presented in the following section s of this report.

3D MEMORY MATERIALS

1. SP

One of the rather promising class of molecules which have been used in basic experiments for 3D storage are the spiropyrans (SP). These are molecules of the general structure shown in scheme 1. Their photochromism, namely their change in molecular structure and color after light absorption, is attributed to the photo-induced cleavage of the carbon-oxygen bond of the pyran ring followed by isomerization to another form referred to as merocyanine. Spiropyran molecules are composed of two distinct molecular components linked by a sp^3 hybridized carbon. These two components are positioned orthogonal to each other. In such an orthogonal configuration the π-electron moieties of the molecule do not interact with each other and the effect is a molecule whose spectrum shows a strong band in the UV region and complete absence of absorption in the visible. The spectrum of this molecule, which is of the utmost importance for the writing process, can be thought of as a superposition of the spectra of the two orthogonally situated members. This orthogonal structure is employed as the "write" form of the device and information may be written by two intersecting beams as long as the sum of the two photon energies is equal to or larger than the energy gap between the ground and excited state of this molecule. For SPI the $S_0 - S_1$ energy gap is 350 nm. Light at 350 nm or less induces absorption in this molecule which initiates the photochemical process which induces the opening of the pyran ring forming a new isomer. The open molecule in turn rearranges to planar form as a result of thermal isomerization. This planar form is colored in appearance and absorbs intensely in the 560 nm region, see scheme 1 and table 1.1

$\lambda_{abs} < 400$ nm $\lambda_{abs} \sim 560$ nm
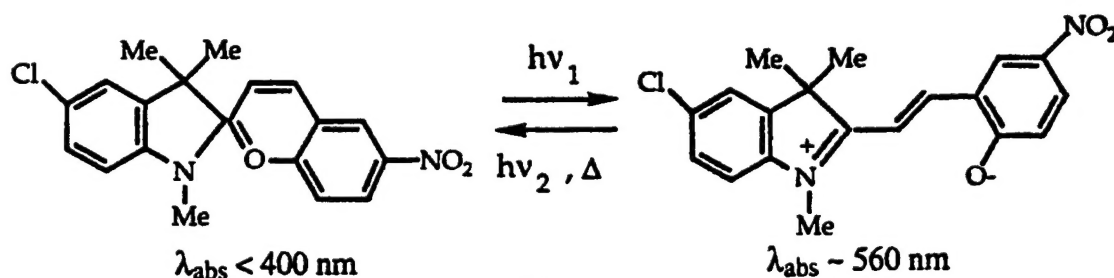
Scheme 1

The colored isomer of the SP molecule is formed with a quantum yield which varies from ~10% to 98%. This variation depend in part on the structure of the original molecule. The energy levels of the chromene and heterocycle components depend upon the substituents and the nature of the environment, i.e. on the solvent or solid matrix. For example, spiropyrans with indoline as the heterocycle components exhibit high quantum yields for photoconversion to the colored forms because of the enhanced intramolecular energy transfer between the two constituent groups. The choice of the molecule used may have, therefore, a profound effect upon the operation, speed and performance of the overall memory device because it dictates the laser power requirements for writing and reading . In addition it determines the lifetime of the photo process, which in essence is the limiting factor of the speed for the input and output of the information to and from the 3D memory device.

1

Table 1.1.

SP	Polymer (Monomer)	Absorption λ_{max} (nm)	Fluorescence λ_{max} (nm)	k sec^{-1}	Φ_{fl}
1	PS	609	645	2×10^{-4}	
	PMMA	580	625	4×10^{-4}	1.6×10^{-2}
	PHEMA	560	605	3×10^{-5}	5.0×10^{-2}
	MMA	580		7×10^{-2}	$< 1 \times 10^{-3}$
	HEMA	560	605	8×10^{-4}	3.0×10^{-3}
2	PS	630	690	6×10^{-4}	
	PMMA	615	670	2×10^{-4}	
3	PMMA	580	620	2×10^{-3}	
4	PMMA	585	605		
5	PMMA	610	610		
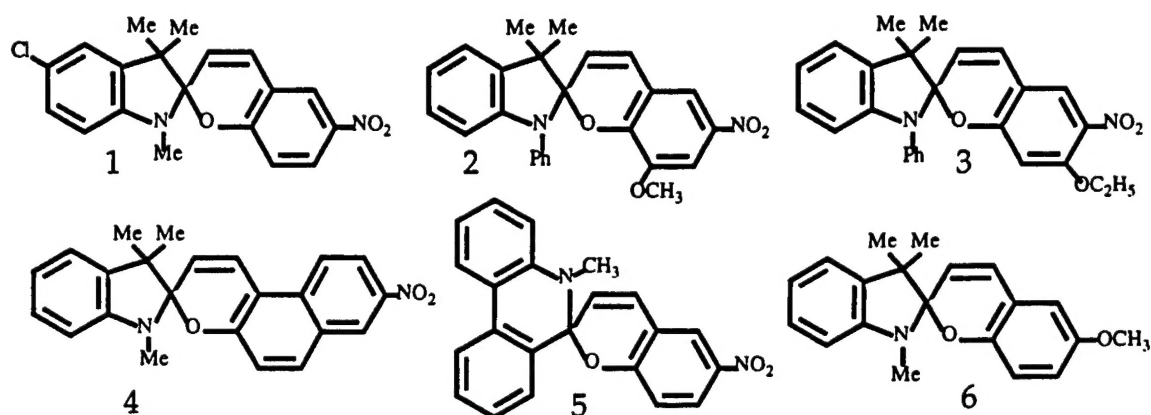
1.1. Experimental system

Absorption and fluorescence spectra were measured on a Shimadzu UV 160U spectrophotometer and Shimadzu FR5000U spectrofluorophotometer. The excitation light sources were either a 150W Ar lamp for slow reactions or a mode locked Quantell Nd/YAG laser for picosecond kinetics and Surelite II Nd/YAG laser for nanosecond studies. Appropriate light filters and monochromators were used to isolate the excitation wavelengths. Determination of the photon flux was achieved by actinometric methods. An accurately measured volume (V) of an Aberchrome 540 solution in toluene at a concentration sufficient to absorb all the incident radiation was exposed to UV light. This solution is placed in a 1 cm optical path cell and irradiated with 316-366 nm light for an accurately known period of time, t. After time t the increase in optical density, ΔD, at 494 nm (the maximum of the long wavelength absorption band of Aberchrome 540) was measured. The photon flux (I_0) may then be calculated from the expression:

$$I_0 = \Delta D_{Act} \; V \; N / \varphi_{Act} \; \varepsilon_{Act} \; l$$

where N is the Avogadro number, φ_{Act} is the quantum yield for the photocoloration of Aberchrome at 540 nm (0.20 for irradiation at 366 nm in toluene) and ε_{Act} is the molar extinction coefficient of the colored form of Aberchrome (8200 dm^{3}mol^{-1}cm^{-1} at 494 nm for the toluene solution) and l is the optical path length.

2

The time resolved experiments were performed with a Nd/YAG picosecond and nanosecond lasers. The picosecond experimental system used for the investigation of the transient absorption spectra and kinetics is shown in figure 1.1.1.
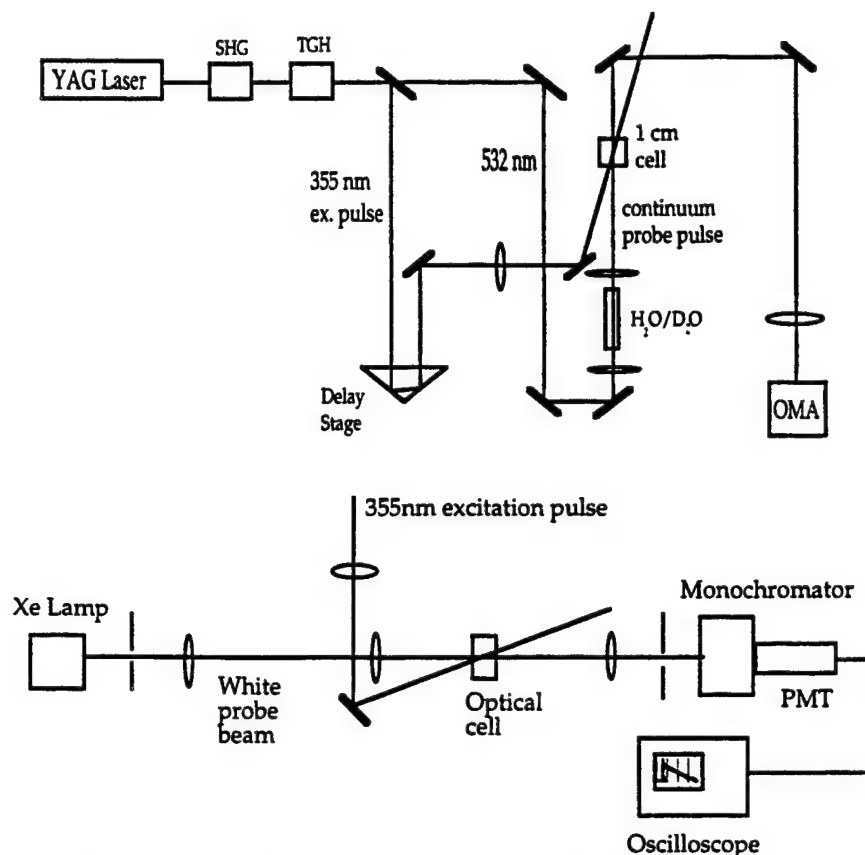
Figure 1.1.1. Experimental System for Transients Absorption Spectra Measurements

A passive/active modelocked Nd+/YAG laser which emits 1064 nm, 25 ps pulses at a repetition rate of 20 Hz provided the laser excitation. The spectra were dispersed using a 0.25 meter polychromator coupled to an OMA system. The energy of the beam was continuously monitored to ascertain that no saturation occured during these studies.

The nanosecond absorption spectra were measured with Surelite II Nd/YAG laser. The spectra were dispersed and recorded by a Jarrell-Ash monochromator and recorded by means of a photomultiplier coupled to a Tektronix 410A digital oscilloscope.

1.2. Mechanizm of write and read process

The mechanism for the "write" and "read" process may be expressed by the following steps:

$$A \xrightarrow{\ 2\,h\nu_1\ } A^*$$

$$A^* \rightleftharpoons I$$

$$I \rightleftharpoons B$$

} write

$$B \xrightarrow{\ 2\,h\nu_2\ } B^*$$

$$B^* \longrightarrow B + h\nu_3$$

} read

$$B \xrightarrow[h\nu_4/\Delta]{} A$$

} erasing
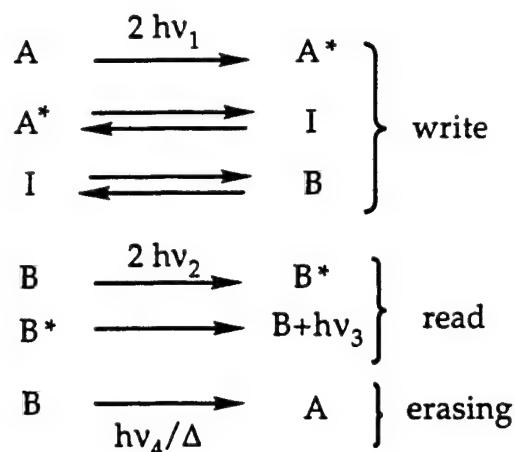
where A represents the original closed "write" form; A^* designates the electronic excited state of A; I is an intermediate species of very short lifetime; $h\nu_1$, $h\nu_2$, and $h\nu_4$ are photon energies; $h\nu_3$ is the fluorescence energy, $\nu_1 \neq \nu_2 \neq \nu_3$ and usually $\nu_1 > \nu_2 > \nu_3$; B is the colored mercocynine, open, "read" form ; B^* designates the excited state of B; Δ = heat.

The speed of the write process depends on the reaction kinetics of the molecule used. In the case of spiropyrans it has been shown that it is a function of the rate of transformation of the closed spiro form to the open merocyanine. Picosecond transient absorption spectra of 6'-OCH_3-indolino-benzospiropyran in toluene reveal (Fig.1.2.1) that, right after excitation with a 25 ps, 355 nm laser pulse, intermediates with absorption maxima in the region of 500-650 nm and 350-450 nm were formed. The absorption intensity of the long wavelength band continued to increase during the first 100 ps, and after that the spectrum remains unaltered for 15 ns.
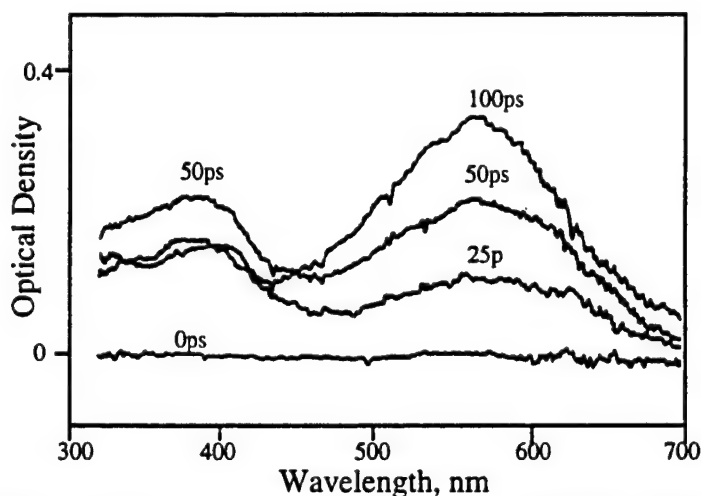
Figure 1.2.1. Transient absorption spectra of SP6 in toluene.

The short wavelength maximum also rises from 0 to 50 ps (practically during in the pulse duration) and after that decreases to a stable value at 100 ps after excitation. There is also a time associated red shift of the short wavelength maximum which shifts from 380 nm at 25 ps, to 405 nm at 100 ps. A decrease in the ratio of the short wavelength maximum intensity to the long wavelength was also observed at 100 ps after irradiation.

The spectra observed and kinetics derived from the experimental data can be explained by the appearance of a cis-cisoid isomer which is characterized by a transient

absorption band with a maximum at ~380 nm. This transient isomer is formed immediately after excitation. After 100 ps it is completely transformed into the stable merocyanine isomer B which shows absorption maxima at 405 and 570 nm. From these data we may conclude that for photochromic spiropyrans the time required for the write process is approximately 100 ps. This is not only the time for writing or reading a single bit but rather is the time required for the simultaneous writing or reading of several pages with Mbt information content each.

1.3. Stability and fluorescence of spiropyran materials

Emission as the principal means for reading the stored information. Because the quantum efficiency of the emission is obviously a very critical parameter for the practical application of this device, we have measured its fluorescence intensity as a function of several parameters such as polarity and hardness of the matrix.

The fluorescence quantum yields of the SP1 written form are presented in table 1.1. The written form exhibits relatively low fluorescence quantum yields, ϕ, ranging from ϕ =3.0 x 10^{-3} to ϕ= 5.0 x 10^{-2} . It was found experimentally that although the emission efficiency of the written form is not very high compared to highly fluorescing dyes, yet the SP1 emission intensity is sufficient to be easily detected from within the 3D volume memory device. One reason for the low emission intensity of these materials is that the rate of the isomerization processes, which precedes the emission, is rather fast or comparable to the fluorescence rate, thus allows it to compete quite successfully with the emission process and hence decrease the fluorescence quantum efficiency. When polar solvents are added they stabilize the polar structure of the written form and consequently decrease the rate for isomerization. Hard polymer matrices also inhibit the large molecular group motion and limit the ability of the SP written form to reverse itself to the original form. As a result, the fluorescence efficiency of the "written" form increases and the stability of the "written" form is greatly enhanced.

The original, "write" form of SP materials which corresponds to zero in the binary code is stable, however, the written form is rather unstable and was found to revert to the original form after a few hours at room temperature. The rate constants for this thermal destruction of the "written" forms of several molecules are listed in table 1.1. The most direct and simplest means for stabilizing this structure is to lower the temperature bellow the activation energy, however owing to fact that the activation energy requires temperatures below minus 30°C stabilization will require cooling to an extent that might not be practical. Because the open form is essentially a di-anion, with a positive charge located on the nitrogen and a negative on the oxygen, an ionic species, such as an acid, could bind these two polar end groups and anchor the molecule permanently onto the open, written structure. This type of stabilization was achieved by the use of HCl and a variety of organic and inorganic acids. The stabilization was modulated by the effectiveness of the reaction and the solubility of the products. The reaction of SP with HCl was found to shift the equilibrium from favoring the closed form to the open form. This has the effect of making the open form indefinitely stable , at room temperature. It was also possible by irradiation with visible light to erase the written bits of information by reversing the reaction back to the closed form. The difficulty with using this acid stabilization process is the low solubility of the bridged material which limits the number of molecules per unit volume. Attempts to increase the concentration have resulted in crystallization of the chromophore in the matrix which in turn make the sample susceptible to high light scattering and therefore renders it unacceptable as an optical device.

2. Naphthaquinones

The optimum case is achieved when the written information is stored for long periods of time, and the materials used have both their "write" and "read" forms stable at room temperature. The "write" form is usually stable, however the open forms of spiropyrans normally undergo reversible cyclization at room temperature which limits long term storage in these materials.
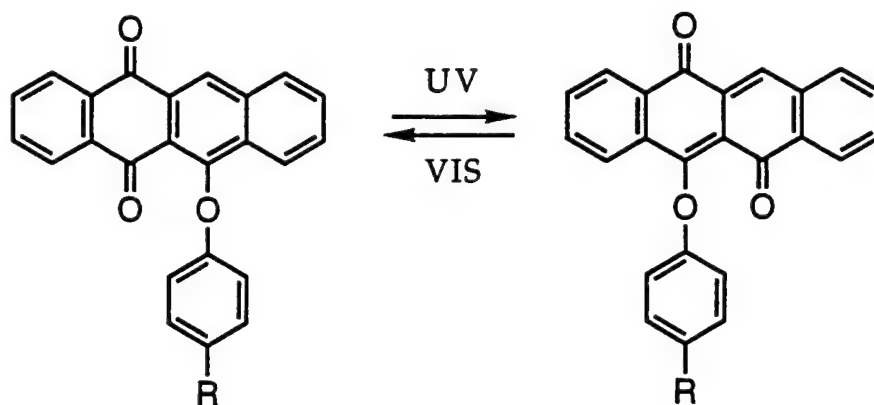
I: R=H; II: R=-CH$_2$-CH(COOC$_4$H$_9$)(NHCOOC(CH$_3$)$_3$)

A desirable property which distinguishes the naphthacenequinones from the spiropyrans is the absence of the back thermal reaction which is responsible for the instability of the colored form of the spiropyrans. Therefore the information storage is permanent at room temperature. This feature, namely the stability of both photochromic forms suggests that photochromic naphthacenequinones may be suitable for use as materials for optical devices and possibly are capable of storing information in 3D devices indefinitely.

2.1. Quantum yields and steady-state kinetics.

Solutions of I and II in degassed benzene, toluene and i-PrOH were irradiated at 405, 366 or 313 nm. The irradiation produced the colored form, B, of I and II respectively which is shown in fig.2.1.1. These colored forms have their absorption in the region of 410-500 nm, are stable and do not revert to the original form at room temperature. The thermal stability of both forms, original, A, and colored, B, is an important property of naphthacenequinones which is absent in the case with spiropyrans where the merocyanine form undergoes thermal back reaction at room temperature. The back reaction can be initiated photochemically by irradiation of the colored form of the naphthcenequinones at 420-520 nm. Prolonged irradiation, several hours, of solutions I and II however was found to generate irreversible decomposition products.

The rate of decomposition was found to be much faster in i-PrOH than in toluene solutions, which suggests that if the irreversible photodecomposition of I in toluene, due to irradiation at 405 nm, is neglected, the general scheme of the phototransformation can be simplified and described as:

$$A \underset{h\nu_2}{\overset{h\nu_1}{\rightleftharpoons}} B \tag{1}$$

Under continuous irradiation the change in concentration of the photoinduced form B can be written as:

6

$$d[B]/dt = I_0[\varphi_B \varepsilon_A f(D)[A] - \varphi_A \varepsilon_B f(D)[B]] \qquad (2)$$

where φ_B and φ_A are quantum yields of the photoprocesses A--->B and B--->A respectively, e_A and e_B are the extinction coefficients of the A and B at the irradiation wavelength, and f(D) and D are defined as

$$f(D) = (1 - 10^{-D})/D; \quad D = \varepsilon_A l [A] + \varepsilon_B l [B] \qquad (3)$$

Equation (2) can be integrated only under the conditions that the optical density of the solution at the excitation wavelength, does not change its value during the time of illumination. Figure 2.1.1 shows that this condition is fulfilled at the~365 nm and~395 nm isobestic points. Under irradiation with 365 nm light and the low conversion efficiencies of A to B eq. (2) can be solved:

$$\varphi_B = [B]/(I_0 t f(D) C_0 e_A) \qquad (4)$$

where C_0 is the concentration at zero time. It can be seen from (fig.2.1.2) that a linear dependence exists between D_B and t, which suggests that the quantum yield φ_A can be determined from the data shown in fig.2.1.1.
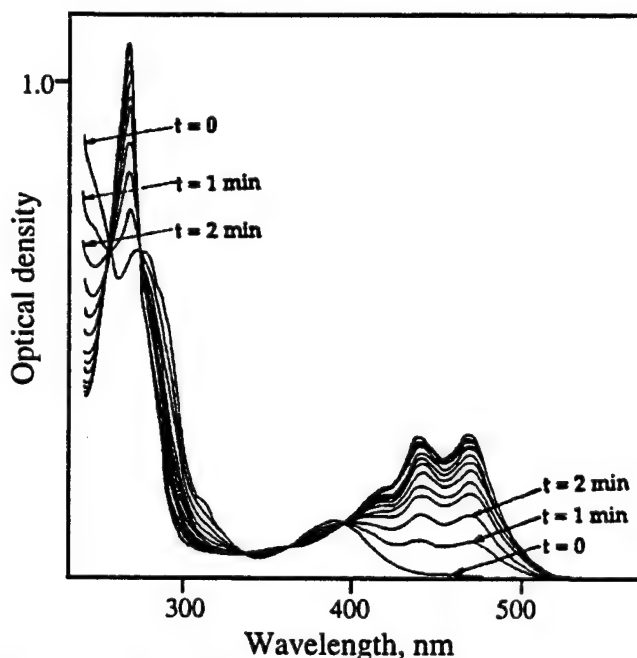
Figure 2.1.1. Absorption spectra of II in toluene. The curves represent the absorbance changes as a function of irradiation time.

     Continuous irradiation of form B by visible light induced also irreversible decomposition. This irreversible decomposition is found, as in the previous case, to be much faster in i-PrOH, than in toluene solution. These results are shown in fig.2.1.3. The rate of photocoloration of I and II in the presence of a small concentration of i-PrOH follows a linear dependence as a function of time. In pure i-PrOH however, a chain reaction takes over and the change in optical density occurs after the irradiation has stoped. The form B fluorescence does not originate from the *ana*-form of B, because UV light

irradiation of the photoinduced form B leads to an increase in the fluorescence intensity. This fluorescence isatributed to the 11-hydroxy-5,12-naphthacenequinone, which is the product of the irreversible decomposition of I. Photodecomposition of both compounds is found to be accompanied by an increase in the fluorescence intensity of the products and this intensity was found to be a linear function of irradiation time. The photoinduced formation of the fluorescing product, which strictly follows the irreversible decomposition of I and II, provides a more sensitive means for investigating the process of decomposition. This data also show that the quantum yield of the photodecomposition is linearly dependent on the incident light intensity . These facts indicate that the decomposition is not the result of secondary photochemistry of the B form but that the decomposition can compete with the main photochromic reaction which results in the structural transformation of the molecule which is responsible for the characteristic photocoloration observed in these materials. Quantum yields of photocoloration and irreversible decomposition are listed in table 2.1.
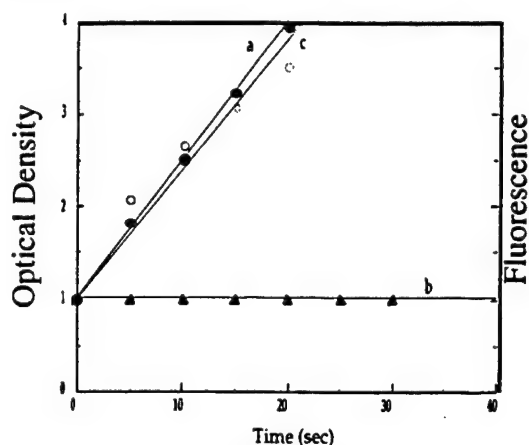
Figure 2.1.2. Normalized OD vs. t for I in toluene measured at 480 nm and at the isobestic point at 395 nm shown as lines a and b respectively. 2c Is a plot of relative fluorescence intensity as a function of time measured at λ_{max}= 540 nm, λ_{exc}=480 nm.
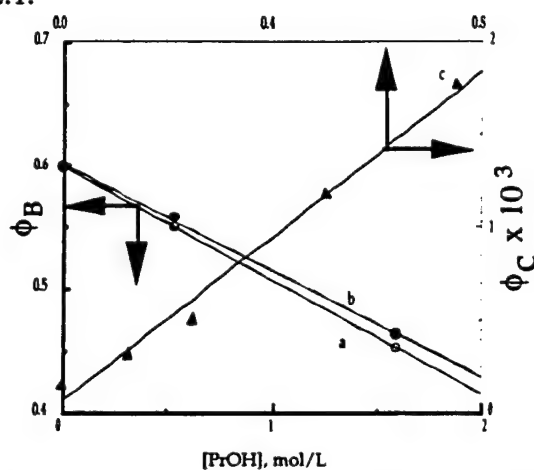
Figure 2.1.3. Dependence of quantum yield on added concentration of i-PrOH in solution of I and II in benzene.a: for the reaction A---> B of I;b: for the reaction A---> B of II; c: for the irreversible decomposition of I

Table 2.1

Quantum yields, (φ_B), of photochromism and irreversible photodecomposition, (φ_C), of compounds I and II in the presence of oxygen.

n	Solvent	λ exc.	ε_B	φ_B	φ_C
II	Benzene	313	5.40×10^3	0.6±0.1	0.00052±0.0001
II	Benzene	366	(455 nm)	0.6±0.1	0.00034±0.0001
II	""	405		0.58±0.1	0.00021±0.00006
II	i-PrOH	313	-	0.45±0.1	0.0069±0.0001
II	""	366		0.4±0.1	0.0026±0.0001
II	""	405		-	-
I	Benzene	347	1.7×10^4	0.6	-
I	Benzene	366	(480 nm)	0.6±0.1	0.00014
I	i-PrOH	366	-	0.5±0.1	0.0035±0.0005

8

2.2. Photochemical reactions and transient kinetics

2.2.1. Picosecond excitation. Solutions of I and II in toluene and in i-PrOH were irradiated with 355 nm, 25 ps pulses. The time resolved, from 0 to 17 ns, absorption spectra, obtained in the 300-600 nm region, following 355 nm excitation are shown in figure 2.2.1.1. The absorption band located at ~ 380 nm decays with a fast rate during the first 75 ps. Analysis of data makes it obvious that the primary absorption (λ_{max} ~ 380 nm) decreases while the red-shifted secondary absorption band (λ_{max} ~ 500 nm) grows simultaneously with the same rate. In order to investigate the kinetic behavior of the transients produced by the excitation of I and II, their absorption intensities changes were measured as a function of time. A plot of the change in intensity of the transient vs. time, shows the decay of the secondary absorption band intensity, λ_{max} ~ 500 nm, at various time intervals between 0.1 and 14 ns. The formation and decay of the transients states of I, are plotted in fig. 2.2.1.1.

When a solution of I in i-PrOH was irradiated with 355 nm pulses, we observed that the decay rate of the secondary absorption band, (λ_{max} ~ 500 nm), became much faster in comparison to the rate of I in toluene. These data are shown in fig.2.2.1.2.
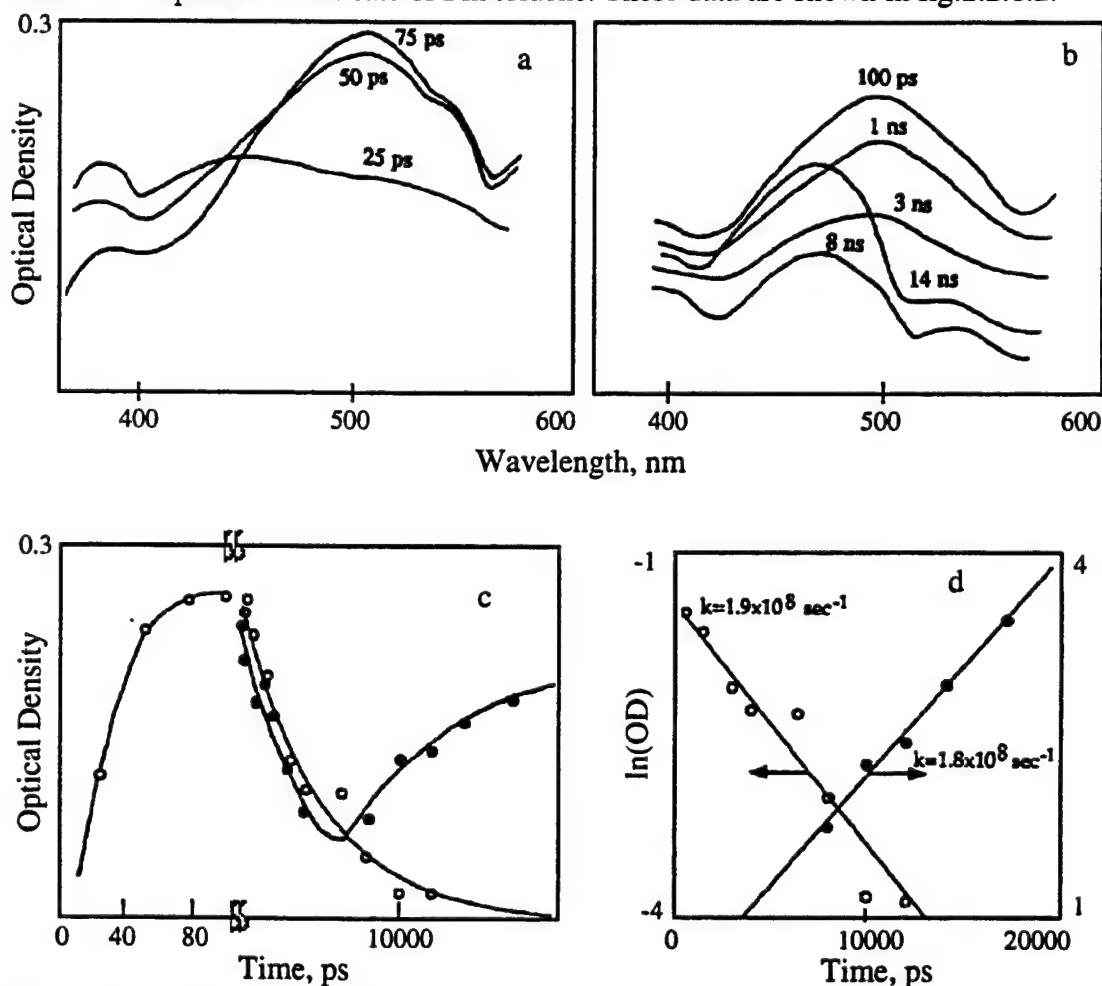
Figure 2.2.1.1.Time resolved transient absorption spectra and kinetics of I in toluene (4x10^{-4} M), excited with a 25 ps 355 nm pulse. **a** and **b**: Transient spectra . **c**: Open circle, kinetics measured at 500 nm. **c**: Closed circles, kinetics measured at 460 nm. **d**: Rates of decay and formation.

9
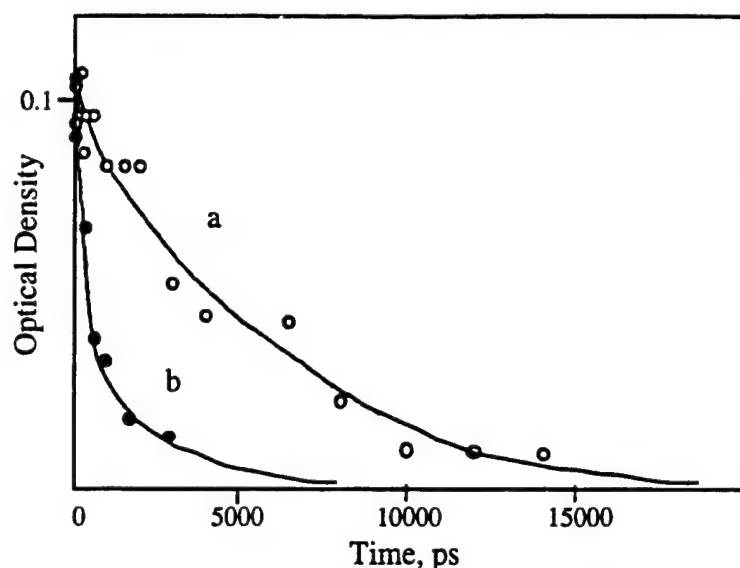
Figure 2.2.1.2. Optical density ($\lambda = 500$ nm) vs time for the transient IA in toluene and isopropanol curves a and b respectively.

2.2.2. Nanosecond excitation. When a deoxygenated solution of I in toluene was excited with 8 ns pulses we found that a transient species, with an absorption spectrum which has its $\lambda_{max} \sim 400$ and 460 nm was formed within the eight nanosecond time period of the excitation pulse. Time resolved spectroscopy revealed a decrease in the 400 nm absorption band intensity, which was also accompanied by a rise in the absorption of a photoinduced stable product of I. The absorption at 470 nm is assigned to the photoinduced *ana*-form of I, because it is stable and has the same spectrum as the *ana* form. The change in the spectra of the intermediate form occuring immediately after excitation with a nanosecond pulse and 50 ms after excitation are displayed in fig.2.2.2.1.
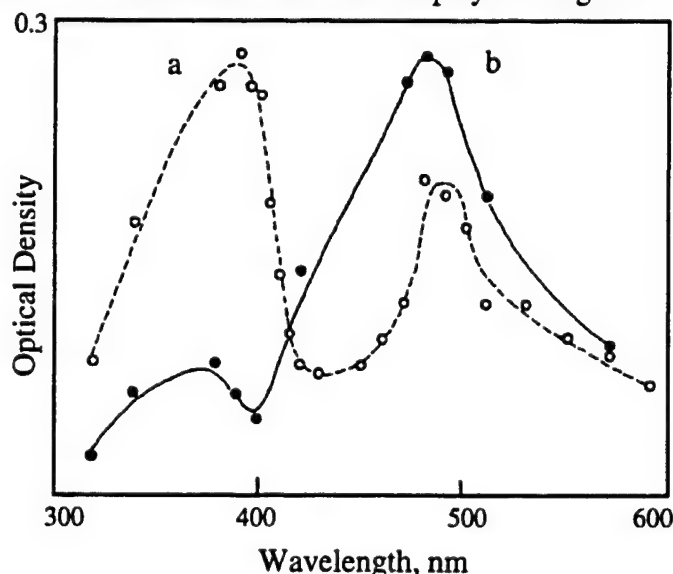
Figure 2.2.2.1.Triplet-triplet absorption spectra of I in toluene: a) immediately after nanosecond excitation. b) 50 µs after excitation

In the presence of oxygen the decay time constant of the first transient and the rise time of the *ana*-form become respectively faster, but the quantum yield of the

10

photoinduced form remains the same as it was in the absence of oxygen. Pulse excitation of IB and IIB in toluene with visible light leads to the same transient with $\lambda_{max} \sim 400$ nm and its decay rate is also found to be increased by the presence of i-PrOH.

2.2.3. Mechanism of photoreactions.

On the basis of our kinetic, time resolved specroscopic data and the information available in the literature, we have been able to assign the time constants we have measured to specific processes and the transient spectra to specific intermediate species. These assignments allow us to propose a most probable mechanism for the photochemical reactions leading to the formation of the *ana*-form of the naphthacenequinones studied. If we start the analysis of the mechanism by considering the final, stable product, B we propose that:

The stable *ana*-form of I could be formed from the transient species with $\lambda_{max} \sim 400$ nm. This precursor of IB is a triplet: it has a lifetime of about 30 ms in the absence of oxygen and it is quenched by oxygen. However, the quantum yield of B does not depend on the concentration of oxygen. This statement is based on both the quantum yields and the kinetic data. Therefore the precursor of B, whose spectrum has a $\lambda_{max} \sim 400$ nm must be the triplet state of B. Subsequently, the quenching of this triplet state leads to the ground state of B. Direct excitation of B induces a triplet state population which leads to the observed triplet-triplet absorption of B. The molecules in the triplet state B may then interact with i-PrOH to abstract an H-atom.

The triplet state of B could also be formed from its singlet state or in fact from another triplet state. As can be seen from fig. 2.2.1.1 the transient species with $\lambda_{max} \sim 400$ nm and ~ 460 nm is formed from the secondary transient with a rate constant $\sim 1.8 \times 10^{8} s^{-1}$ and an absorption spectrum with $\lambda_{max} \sim 500$ nm.

The next task is to analyze the nature of this transient species whose spectrum is characterized by an absorption band with a $\lambda_{max} \sim 500$ nm. This spectrum coincides with that of the triplet-triplet absorption of the non-photochromic 5,12-naphthacenequinone in the same solvent. The decay of the 380 nm band, of compound II, corresponds to the population decay of singlet, $(A)S_1$ to the triplet, $(A)T_1$ ($\lambda_{max} = 500$ nm) which proceeds with a lifetime of 8.3×10^{-11} s. The triplet state of A decays to the triplet state of the B form, $(B)T_1$, (λ max=400 nm and 460 nm), with a lifetime of 8.3×10^{-9} s. The B form triplet decays into the final product B with a lifetime of 6.3×10^{-6} s.

It is quite reasonable therefore to assume that the transient with $\lambda_{max} \sim 500$ nm is the triplet state of A, i.e. the initial quinoid form of I and II. This triplet state is capable of abstracting a hydrogen atom from i-PrOH because the decay of this triplet is accelerated in i-PrOH. The process by which a triplet state of A is formed, with a rate constant of 1.2×10^{10} s^{-1}, actually represents the intersystem crossing rate in A.

Based on our kinetic data the most probable mechanism for the formation of the photochromic product, induced by the 355 nm excitation of I and II, may be represented as follows:

$$
\begin{array}{ccccccc}
 & & k_1=1.2\times10^{10} & & k_2=1.8\times10^8 & & k_3=1.6\times10^5 \\
A + h\nu \longrightarrow & A(S_1) \rightsquigarrow & A(T_1) \rightsquigarrow & B(T_1) \rightsquigarrow & B \\
\lambda_{max} = & 380 \text{ nm} & 500 \text{ nm} & 400, 460 \text{ nm} & 490 \text{ nm}
\end{array}
$$
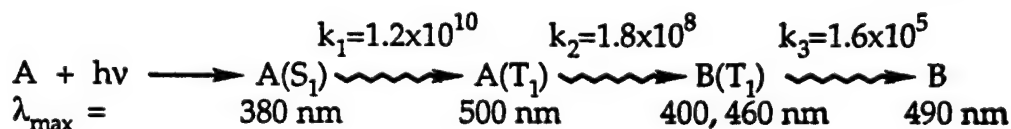
We may propose, therefore, that the photoisomerization reaction of photochromic naphthacenequinones I and II is an adiabatic photoreaction proceeding via the triplet state.

11

The existence of triplet ketone intermediates suggests that H-atom abstraction could compete efficiently with the photochromic reactions. It follows from the above scheme that the formation of B (φ_B=0.6) is directly related to the decay of B(T$_1$). However the H-atom abstraction could also compete with the photochromic reaction (1). Steady state experiments show that in the presence of i-PrOH the quantum yield of the photochromic reaction decreases and the quantum yield of the irreversible photodecomposition reaction of B increases. In terms of this scheme it is reasonable to assume that the irreversible photodecomposition is driven by triplet B state H-abstraction . Reaction (4) represents the irreversible decomposition by hydrogen abstraction from the solvent.

$$B(T_1) \longrightarrow B(S_o) \tag{1}$$
$$B(T_1) + i\text{-PrOH} \longrightarrow BH\cdot + (CH_3)_2COH\cdot \quad \text{irreversible decomposition} \tag{2}$$
$$B(T_1) + O_2 \longrightarrow B(S_o) \tag{3}$$
$$B(T_1) + RH \longrightarrow BH\cdot + R\cdot \tag{4}$$

Using the above reaction scheme for the addition of i-PrOH we can write the following expression which relates the quantum yield of the photochromic reaction with the concentration of i-PrOH.

$$(\varphi_B)_o/\varphi_B = 1 + \tau_B k_4[i\text{-PrOH}]$$

where $(\varphi_B)_o$ and φ_B are the quantum yields of photocoloration in the absence and in the presence of i-PrOH and t$_B$ is the lifetime of the lowest triplet state B(T$_1$). A plot of φ_B versus [i-PrOH], shown in fig. 2.1.3, suggest that they are a linearly related. We also found that $k_4 = (5.1\pm0.6)10^4$ M^{-1}s^{-1} for compound II in benzene. Time resolved experiments confirm these results because they give the rate constant for the direct quenching of B(T$_1$) by i-PrOH as $(9.3\pm0.7)10^4$M^{-1}s^{-1}.

Considering this scheme the following relationship is proposed for the quantum yield of the irreversible decomposition:

$$\varphi_B/(\varphi_C)_o = \{k_4[i\text{-PrOH}] + k_6[RH]\}/\{k_6[RH]\tau_B(1/\tau_B + k_4[i\text{-PrOH}])\}$$

Assuming that $k_6[RH] = 139$ s^{-1}, in benzene we obtain $k_4 = (4\pm1)10^3$M^{-1}s^{-1}. The lower value for the decomposition compared to the photocoloration data plotted in fig.2.1.3 can be explained by the partial reversibility of reaction (2).Therefore, the largest rate constant possible under this scheme, for the H-atom abstraction by B(T$_1$) of II in benzene is $(9.3\pm0.7)10^4$M^{-1}s^{-1}. Such low rate constants for H-abstraction from i-PrOH are characteristic of a triplet π,π^*-state. The rate constant of the H-atom abstraction by A(T$_1$) of II is found to be more than 1.3×10^8M^{-1}s^{-1}, which is characteristic of a triplet n,π^*-state. Based on this kinetic and spectroscopic data, the lowest triplet state may therefore be assigned to n,π^* in 5,12-naphthacenequinone form A and π,π^* in form B.

In summary, time resolved spectra and kinetic data have made it possible to assign the spectra of the intermediate species, measure the formation and decay of the transient states of naphthacenequinones and propose a mechanism for the reactions and photochemistry responsible for the photochromism of these materials.

2.2.4. Fluorescing naphthacenequinones.

Photochromic naphtacenequinones have both write and read forms stable at room temperature. This is a property which makes them promising materials for 3D memory devices, but they also lack fluorescence in either form. Because of the absence of fluorescence the information cannot be read by means of light emission from the bits being read.

The new naphthacenequinone type molecules combine high fluorescence intensity with stability of both forms at room temperature. Therefore, they are very promising memory materials.We have synthesized several new materials of this structure. All materials were dispersed in PMMA polymer matrices and their absorption and emission properties were studied in detail. Some of these materials have photochromic properties, i.e. ability to revert to another form, which has a different spectrum and color when excited by light.
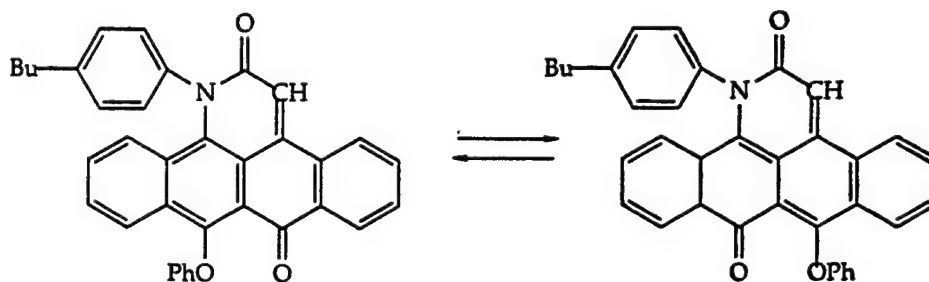
Figure 2.2.4.1. Photochromic naphthacenequinone based material with fluorescing written form.

A typical material with this structure is presented in fig.2.2.4.1. It consists of two forms, which are interchanged by light excitation. Both forms were found to be stable at room temperature. And accelerated stability tests suggest that the written information will remain unaltered for several months. The written form was found to emit fluorescence at λ_{max}=560nm with a sufficient high quantum efficiency to be used for reading information with ease. Absorption spectra of both write and read forms are shown in figure 2.2.4.2.
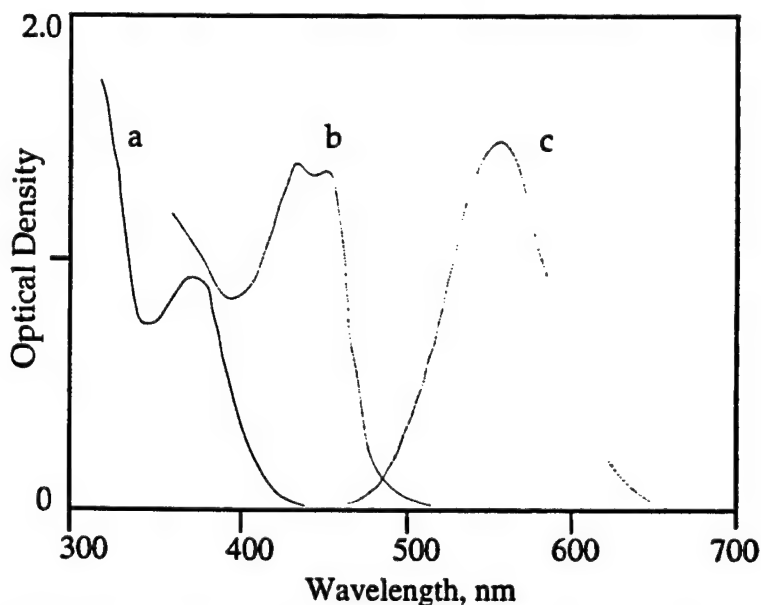
Figure 2.2.4.2. Absorption spectra of the a)write; b)written forms and fluorescence spectrum c) of the written form.

13

We studied also the reversibility and fatigue of these naphthacenequine materials, which is a very important characteristic if information is to be written read and erased many times. The degradation of the material was observed after a few cycles and the efficiency of this destructive irreversible processes was found to be very high. This degradation of the material under UV irradiation will significantly limit practical application of this material in memory and other optical devices. Even though this particular material cannot be erased without damage to the material it can be used as archival memory.

3. Fulgides
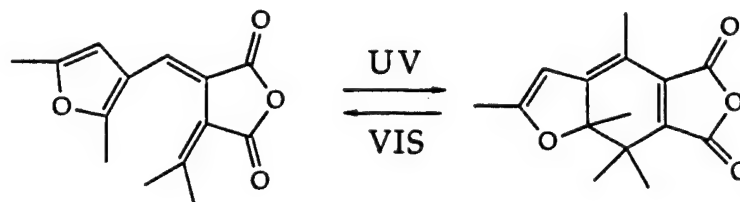
Figure 3.1. Chemical structure of photochromic fulgide

One of the new photochromic materials studied are fulgides, which have the chemical structure shown on fig.3.1. It was found that fulgides embedded in PMMA matrices can have two distinct forms, colorless and colored, which can be transferred from one to another by means of light excitation. These two forms correspond to "write" and "read" forms respectively. Fulgides were found to be stable at room temperature in PMMA matrices and the written form was stable for at least two months. The absorption spectra of the write and read forms are shown in fig.3.2.
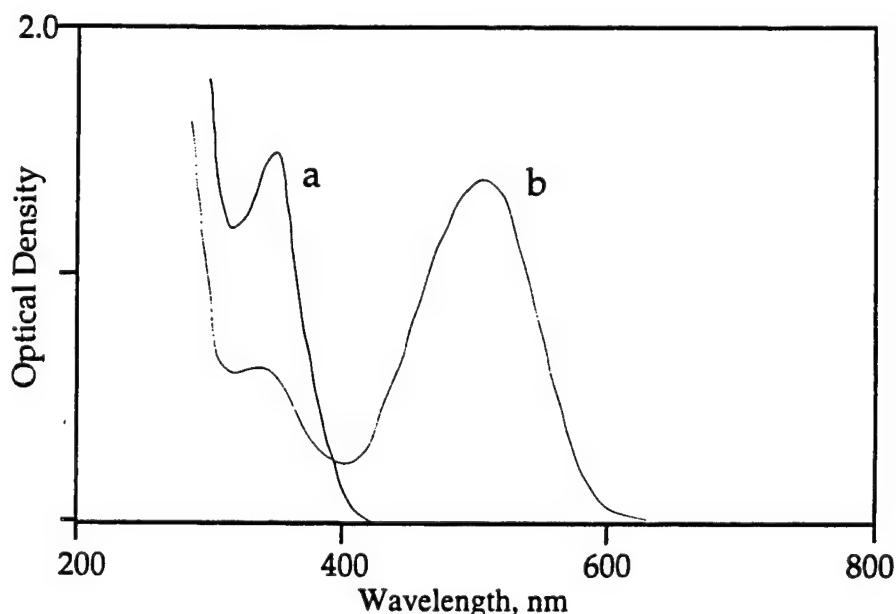
Figure 3.2. Absorption spectra of write, a, and written, b, forms.

The spectra indicate that the writing of information must be done by 630 nm laser pulses. Because the laser available does not emit at this wavelength and neither the SHG of Nd/YAG is suitable, SHG $\lambda = 532$ nm, we designed a new system, which converted the 532 nm SHG into 630 nm pulses by means of Stimulated Raman Scattering (SRS). The

14

medium used for generating 630 nm SRS pulses was a 1 meter long cell filled with methane, CH_4 at 25 atm pressure.

Attempts to utilize two beams with wavelengths 1064 nm and 532 nm for two-photon writing were not successful, possibly due to the rather effective erasing process induced by the one-photon absorption of the 532 nm photon owing to the high absorption cross-section at 532 nm.

We also studied the fluorescence properties of these photochromic fulgides. However, the experiment showed that fulgides with the structure shown in fig.3.1 do not fluoresce in either liquid solutions or when embedded in solid polymer matrices. The absence of fluorescence limits their application in devices where the reading process is based on emission detection.

We have investigated several means which may make possible the modification of the chemical structure of these molecules in order that one of the forms will have fluorescence. We discovered that new indoline based substituted fulgides when dispersed in PMMA matrix are photochromic and exhibit two forms both stable at room temperature. They convert to the write form with absorption at 400 nm, and read form with absorption at ~510 nm. We modified these compounds so that in the read form this class of fulgides emits fluorescence. The fact that both forms are stable at room temperature and the read form fluoresces strongly suggests that they are suitable memory materials.

4. Dimer materials

We previously reported that dimer-monomer materials show very high stability of both write and read forms at room temperature and high emission efficiency. We studied the possibility of shifting the spectral region to a more convenient wavelength, of these systems by using different monomer molecules and varied the mechanism for the transformation between dimer and monomer, or write and read forms.

2-Aminopyridine forms the dimer molecules, when excited by light with wavelength ~300 nm. Crystals of the dimer were grown then dispersed in polymer, which were then molded into cubes and subsequently they were polished to optical quality. Information was written inside the volume of the cube by means of excitation of the dimer with two-photon 532 nm photons. Excitation leads to the formation of the monomer, which is the written form. This form has its absorption maximum at 300 nm. This form has also intense high quantum yield fluorescence with its maximum wavelength at 370 nm. The solubility of these molecules is better than that of anthracene and 9-methylanthracene, which we reported previously, therefore a larger number of molecules per unit volume are available for information storage resulting in a higher signal and more written bits per unit volume. In addition, the high molecule concentration affords for lower laser power required for storing and retrieving information.

The write forms, namely the dimers of 2-aminopyridine and anthracene, have absorption below 300 nm and therefore writing in this case, may be achieved by utilizing 2-photon absorption by means of two 532 nm beams. The utilization of two beams of Nd-YAG laser emitting at 1064 and 532 nm wavelengths respectively allows for better signal to noise ratio. However, in order to use these two wavelengths we need to shift the absorption spectra of the write form to the region of 355 nm, which is the sum of two photon energies with 1064 and 532 nm. This entails the synthesis of new materials with the appropriate chromophoric groups to shift the absorption. To achieve this we tried to use the system based on tetracene dimer-monomer combination. The dimer of tetracene was obtained by excitation of deoxygenated solutions of monomer with visible light. The precipitated dimer was collected, purified and dispersed in a polymer matrix to produce the photochromic memory device. The absorption spectra of the write form of this material was red shifted compared to anthracene. As planned the two absorption maxima of the dimer occur at the region of 355 nm, making it possible to write the information by a 1064 nm and a 532 nm picosecond laser beams. Unfortunately, the solubility of this molecule was

very low and it was not possible to create a sufficiently high concentration for the two-photon process to be effective. It was also found that, for this system, in the presence of oxygen, oxidation and other irreversible processes are very effective and coupled with its low solubility of this material in most polymer host matrices is deemed to be not suitable for practical application in 3D-memory devices. We are experimenting with other dimer monomer systems which have better characteristics and thus are more suitable for 3D devices.

To understand the mechanism which is driving the write and read processes and estimate the rate of writing and reading in 3D format using these materials, we studied the transient states and species occurring during the writing and reading processes. We also devoted a considerable period of time and effort in understanding the mechanism and kinetics from cw to the picosecond regime. To this effect we have identified all the transient absorption spectra and kinetics of anthracene and 9-methylanthracene dimers and monomers in solution and condense phase. Our experimental data show that excitation of the dimers leads to the appearance of short lived transients. The decay kinetics of these transients were found to follow first-order kinetics with a lifetime of approximately 3 ns, while the accumulation of new transients with absorption maximum at 430 nm was observed. Based on our data, we may conclude that the write process, which is actually the dissociation of the dimer, proceeds via the formation of the excimer, which is an ultrafast intermediate molecular species in the excited electronic state. When the excimer relaxes it dissociates into two molecules of monomer, namely the written form: one remains for awhile in the excited triplet state with a characteristic absorption band at 430 nm and the other decays directly to the ground state. The speed of the write process is characterized by the appearance of the written form which occurs with a rate of $\sim 3 \times 10^8$ or a 3×10^{-9} lifetime. The relaxation of the triplet state monomer leads to the additional accumulation of the written form with nanoosecond rate. The speed of the reading process is determined by the lifetime of the fluorescing first electronic excited singlet state of the monomer molecule. Experimental data performed in solution and solid matrices show that the fluorescence decay with a lifetime of ~ 2.5 ns.

5. Hexatrienes

We studied the new photochromic material as a possible component for construction of an erasable, stable 3D memory device. Our experimental data show that a number of hexatriene compounds undergo reversible photochemical isomerization which results in the changes of the absorption spectrum. The basic mechanism responsible for this chemical structure change may be represented as the following:
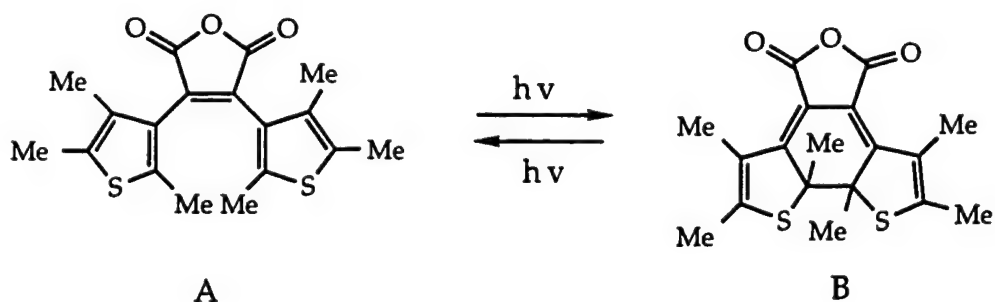
Scheme 1

We found, that some of these compounds may exhibit desirable properties such as thermal stability of both forms, fluorescence and reversibility, which are mandatory properties for utilization in rewritable optical memory. The material, shown in scheme 1,

named 2,3 Bis (2,4,5-trimethyl-3-tienyl)-maleic Anhydride changes its color when excited by light at λ =355 nm. The changes in the absorption spectra taking place after excitation are shown in figure 5.1. The absorption spectra of the two forms of that material, which are designated as "write" (A) and "read" (B) respectively, are considerably different in shape and intensity and are well separated. The "write" form has its long wavelength absorption in the region of 300-400 nm excitation at this wavelength by two photon absorption; fundamental and second harmonic of the Nd-YAG laser reduces for B, scheme 1. The absorption spectrum of the written form is shifted to the red region compared to the A form with a long wavelength band absorption at 500-600 nm. We found that light excitation in this absorption band leads to discoloration of material due to reversible photoreaction and formation of "read", form (A). Reversible coloration of this material was observed in different liquid solutions and polymer matrices. We studied the thermal stability of both read and write forms at room temperature. PMMA films with dispersed photochromic material were prepared by solvent evaporation from solution of polymer and photochrome in dichloroethane, on microscopic slides. Our experiments show that both write and read forms have excellent stability at room temperature and no changes in absorption spectra were observed during at least one month.
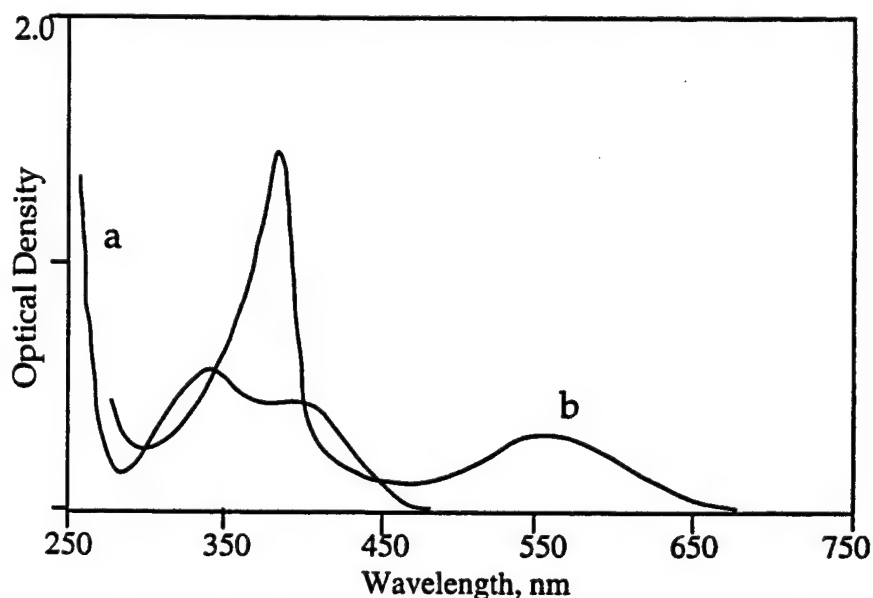
Figure 5.1. Absorption spectra of write, a, and written, b, forms

We studied the fluorescence properties of this new material in various solutions and polymer matrices. Fluorescence of form A is observed when the molecules are excited with UV light.The fluorescence intensity from the sample decreases when part of the form A is transferred to the form B. No fluorescence from the form B of the investigated, 2,3 Bis (2,4,5-trimethyl-3-tienyl)-maleic Anhydride, material was observed, even in polar solvents and polymer matrices. The lack of fluorescence in the colored form makes this material difficult to use in memory systems, because the reading process is based on detection of emission from the written form. Additional modification of the molecular structure, such as attachments of substituents capable of fluorescence, are expected to lead to the appearance of fluorescence.

6. ROM material

17

We developed a new photochromic material to be used in conjunction with 3D memory devices. This new material has its write and read forms stable at room temperature and also permits non destructive reading of information.

The goal of this research, was to construct a new acid stabilized material with two components which working synergistically will provide the properties of stability and intense fluorescence not found in other systems: one component is light sensitive, and the other is the dye precursor, which may react with the products generated by photochemical or reaction of the light sensitive molecule to reproduce a new high quantum yield fluorescing molecule.

During our studies we were able to transform the well known laser dye Rhodamine B to a colorless, nonfluorescing, lactame form by reacting it with a base. This form was determined to be s stable at room temperature and remains unchanged for long periods of time, i.e. months or years. If the acid species is added to this lactame form, it can be transferred back to the Rhodamine colored dye form, which also has very strong fluorescence in the visible region. The fluorescence quantum yield is close to 100%. The absorption spectra of the colorless lactame molecule and the colored forms of Rhodamine B are shown in figure 6.1. The fluorescence spectrum of the colored, read form is shown also in figure 6.1. The absorption spectrum of the dye has absorption maximum at 545 nm and the absorption cross section at the exciting wavelength is $\varepsilon_{532} = 7.2 \times 10^4$.
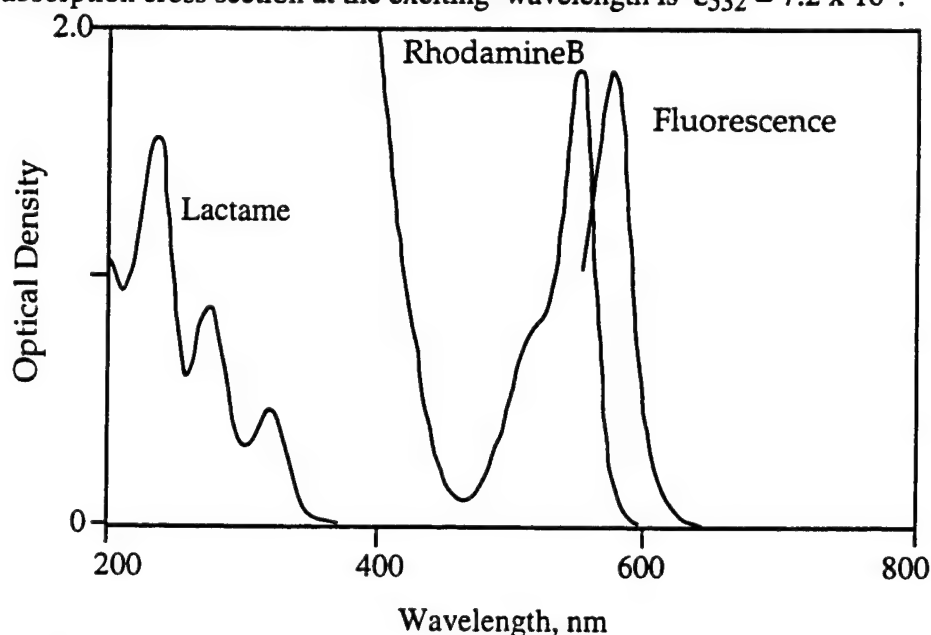
Figure 6.1. Absorption spectra of lactame, Rhodamine B and fluorescence spectrum of Rhodamine B.

This high absorption cross-section value is a very important parameter, because the two photon fluorescence can be easily induced by a rather weak 1064 nm laser beam. This high value suggests that the reading process and much lower power lasers than previous materials necessitated. An additional favorable property of the write form of this material is that it neither absorbs neither fluoresces at wavelengths longer than 350 nm. Therefore the large Stokes shift which occurs between the absorption of the two forms ensures that no writing occurs during the reading process.

We used 2-nitrobenzaldehyde as the photosensitive substance to produce the acid. This material reacts with the colorless lactame form and transforms it to the colored dye read form. 2-nitrobenzaldehyde under UV light excitation undergoes photochemical reaction and produces nitroso-acid. Our experiments show that this acid readily reacts with the colorless lactame form causing its transformation to the colored dye form, as shown in

18

scheme 1. Our study shows that the primary colorless and non-fluorescing solution of lactame becomes highly colored when excited with 355 nm and thereafter it emits intense fluorescence.
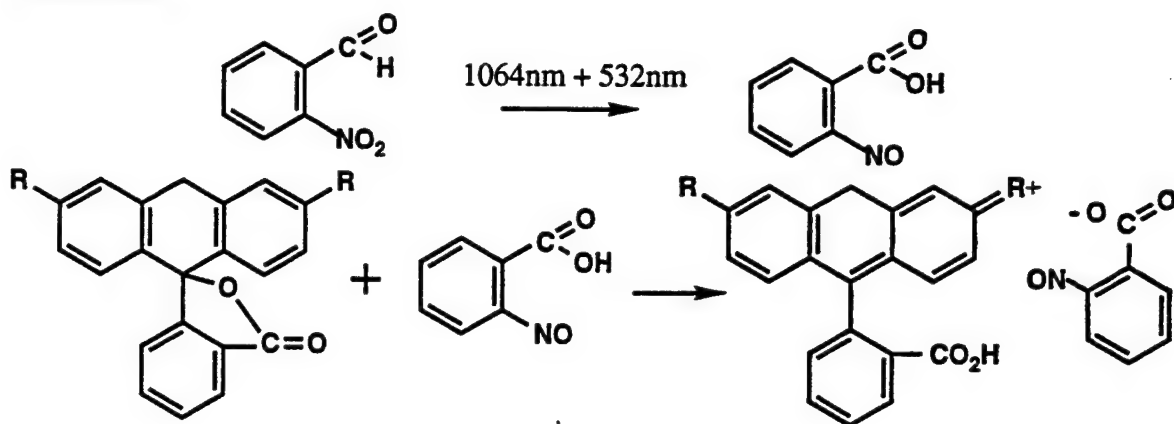
Scheme 1

Scheme 2 shows the write and read processes of this molecular system as will occur in 3D memory devices, based on this bicomponent system. The combination of light sensitive acid generator and colorless dye precursor, lactame become the write form. Both components are stable at room temperature, and no changes were observed in the write form absorption spectra after extended periods of time. The write process involved two steps: first a two photon induced acid formation by the acid generator, and the second step involved the reaction of the acid with the dye precursor and the change of its structure to the colored dye form. The colored dye form is the written form of 3D material and it is also stable at room temperature.

Write Process

532 nm
1064 nm

Acid Generator $\longrightarrow$ Acid

Acid + Dye Precursor $\longrightarrow$ Colored Dye

Read Process

Colored Dye + hv $\longrightarrow$ Fluorescense

532 nm: 1 photon exc.
1064 nm: 2 photon exc.

Scheme 2

19
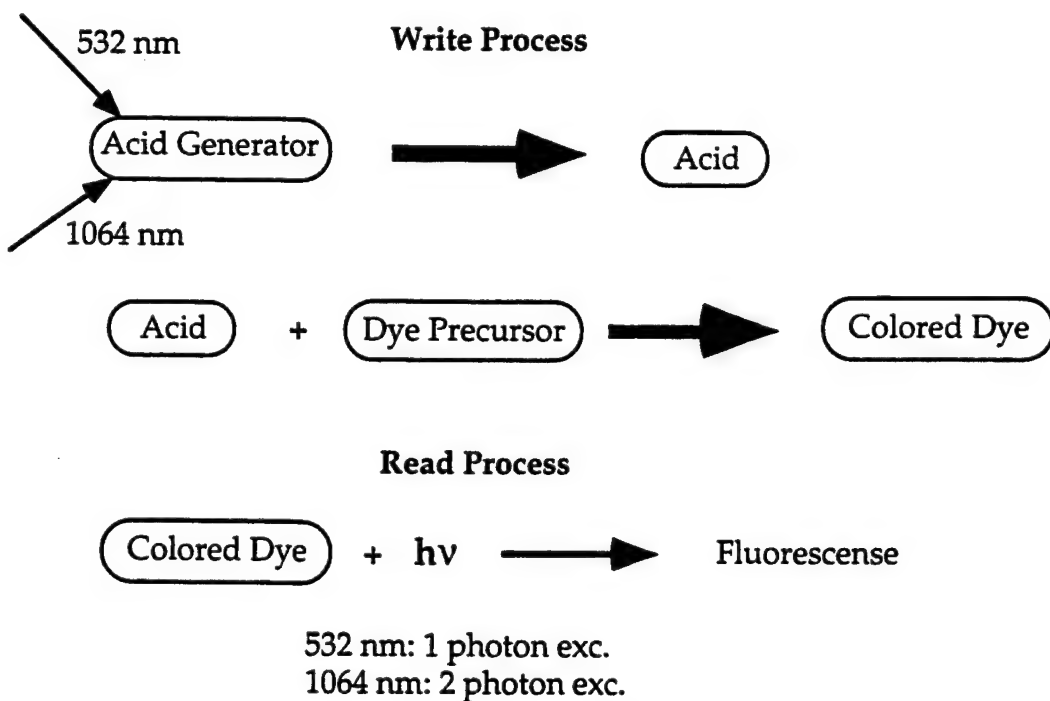
Because the dye, Rhodamine B, is a stable material and does not undergo photo or thermal decomposition, at room temperature, the light used for information reading does not introduce changes in the written form. Read cycles may be performed 10^5 - 10^6 times without any noticeable material decomposition.

6.1. Acid generators.

We explored the suitability of different materials as acid generators, because the absorption cross section of 2-nitrobenzaldehyde is not large enough at 355 nm where two photon excitation, by 1064 nm and 532 nm beams of Nd-YAG laser, to satisfy low power laser utilization.

Several molecular systems were considered as candidates for acid photogeneration. The list of these materials is presented in table 6.1.1. It was determined experimentally that photoinduced acids react with the colorless form of the dye which exhibits intense fluorescence properties in the visible region. It was found, that there is a small background fluorescence in the original material. This initial fluorescence could be due to the presence of traces of acid or water in the compounds, which may subsequently react with the dye precursor to produce small amounts of the read form dye.

Table 2. Photogeneration of Acid

Substance	Absorption, nm	Efficiency, %
dibromoethane	240	200
diiodoethane	260	200
diiodomethane	300	200
aryldiazonium salt	<300	~40
diaryliodonium salt	<300	~40
triarylsulfonium salt	<300	~40
nitrobenzaldehyde	250	60
dinitrobenzaldehyde	250	10
nitronaphthaldehyde	345	~50

The efficiency by which acid is generated varies among the materials investigated with dibromoethane and diiodoethane being as high as 200%. This means that each absorbed photon will produce two molecules of acid. This high yield is possible because of the novel photoreaction mechanism. The high quantum efficiency for acid generation for some of these materials is an important, promising property that can lead to high efficiency in the writing process. Unfortunately, the absorption spectrum of these molecules requires excitation by fourth harmonic 266 nm, of Nd-YAG laser, which makes their practical application slightly more complicated.

6.2. Preparation of high concentration doped polymer blocks.

Our experiments show that the dye precursor has good solubility in most organic solvents including the monomer methyl methacrylate (MMA). The acid generating molecule nitro-benzaldehyde has also very high solubility and can be dissolved in the same materials at concentrations up to 100 mg/ml. This is a very important property because high concentrations of light-sensitive agents are required for the realization of an efficient two-photon process, therefore, low power, small lasers can be utilized. We found that high concentrations of nitro-benzaldehyde decrease the rate of the polymerization process resulting in comparatively soft polymer matrices. The viscosity of these polymer blocks was, however, high enough to prevent the disappearance of the written image by diffusion but the mechanical hardness was not sufficiently large to allow the surface to be highly polished. Nevertheless, these samples exhibit acceptable optical quality while they remain

in the glass cell which was used to disperse the photochromic material in the MMA monomer and subsequently contain the polymerized mixture. We found that such samples could be successfully used in experiments for writing and reading of information without being separated from the glass cell which envelopes it. The optical quality of the surface, in this case, was very good because it was determined by the quality of the glass cell. It is possible, therefore, to achieve very high optical quality samples by using high polished optical quality glass cells.

When the sample preparation time was decreased by increasing temperature, an effect which is known to accelerate the polymerization process, the final polymer product had unacceptable optical properties owing to air bubbles inside the volume. Better quality optical materials were obtained by increasing the initiator concentration and the time of polymerization from 24 to ~ 100 hrs. These samples, prepared by the slower polymerization method exhibit very good optical characteristics and in addition the matrix was hard enough to be polished to ~ 1λ.

Another problem which occurred was the increase in the background color of the samples during the polymerization process, possibly due to some side chemical reactions. It was found, that before polymerization the liquid monomer solution has a slightly yellow color due to the <430 nm absorption band of nitrobenzaldehyde. Essentially no absorption was observed above 540 nm. After polymerization the sample became slightly red colored because small amounts of Rhodamine B dye were formed during polymerization. This dye may also generate a fluorescence background during the reading process. The background fluorescence intensity is considerably lower, than the one induced by the written bits and can be eliminated by background subtraction.

Experiments with two-photon writing and reading of information, inside the polymer cube made with the new photochromic system, show that at the point of intersection of the two orthogonally propagated laser beams with wavelengths 1064 nm and 532 nm, a highly visible spot of the written form was formed with the dimensions of the two overlapping beams. Illumination of the memory cube with green light, 532 nm, reveals that this written spot has considerably brighter fluorescence than the rest of the unwritten volume and can be easily detected by eye or by means of a CCD detector. At the same time, the trace made by the 532 nm beam can also be seen. This trace is the result of two photon absorption from the 532 nm beam as it travels alone within the cube. The energy of two 532 nm photons is the equivalent of one photon excitation by a 266 nm pulse. The nitro-benzaldehyde system has a much stronger absorption cross-section at 266 nm than at 355 nm. This difference in cross-sections leads to increased efficiency for two photon absorption process using 532 nm beam compared to the 532 and 1064 nm two photon process. As a result, the trace from 532 nm beam was observed in the experiments using two 532 nm photons. The utilization of higher energy 1064 nm and lower energy of 532 nm beams for these experiments made possible the increase in signal to noise ratio i.e., spot vs. background. However, we could not completely eliminate background traces owing to the high efficiency of the 532 nm two-photon process. We may resolve this problem by optimization of the laser beams wavelengths or by the utilization of other acid generating materials which have appropriate spectroscopic properties for reading and writing in 3D volume.

6.3. Synthesis and properties of nitro-naphthaldehyde acid generator.

The molecular system which we developed is based upon the binary composition of a dye precursor and a photo induced acid generating molecule. The acid generator in this case is the light sensitive material which is excited by means of two-photon absorption. After a series of excited state transformations, which we are currently studying, the molecule is transformed into the writing form. To be suitable for use with 3D memory devices the acid generating molecules must have the following properties:

a)   The efficiency of the photoprocess which generates the acid should be high i.e. more than 30%.

b)   Both the write and read forms of the 3D material should have a long term (years) stability at room temperature, both in liquid solutions and polymer matrices.

c)   The material should have very high solubility in monomers and the corresponding polymer hosts. The high concentration of the dispersed material will allow for a higher signal to noise ratio and lower laser beam power.

d)   The absorption spectra of the write form should have their maxima in the region of 355 nm in order to perform two-photon excitation with 1064 and 532 nm pulses from Nd/YAG laser.

The substance, which we deduced that would satisfy these conditions, is nitronaphthaldehyde. However, the photochemistry of this molecule is unknown and neither have the spectroscopic and optical properties of this material been reported in the literature. A close analog of this molecule which has been studied is nitrobenzaldehyde which exhibits a red shifted photoproduct which is stable at room temperature. However, this molecule has its absorption maxima of the write and read forms in the UV region which makes this molecule unsuitable for practical devices. Nitronaphthaldehyde is not commercially available, therefore we synthesized it by conducting a two-step organic synthesis.

step 1

step 2
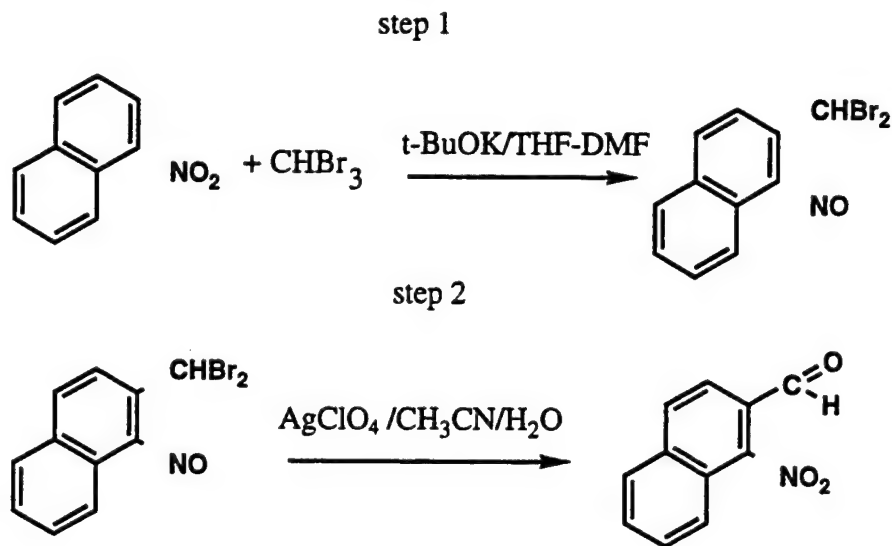
To assure a high yield of the chemical reaction, the first step of this synthesis required low temperature conditions, -70°C, and a small amount of initial reagents. We constructed a low temperature apparatus which utilized solid CO_2 in a temperature controlled Dewar. Because of the thermostat physical dimensions only a small amount of the material could be synthesized at a time. To accumulate a few grams of the final product we had to repeat the initial steps of the reaction about 30 times. The intermediate product was collected and purified by means of chromatography.The second step required refluxing of the reaction mixture under argon atmosphere for about 100 hr., followed by purification of the final product by column chromatography. Using this procedure, we were able to synthesize about 5 grams of the nitronaphthaldehyde compound, which was used in our further experiments for 3D memory recording and reading. The absorption spectrum of this novel material was found to be, as predicted, red shifted in comparison to nitrobenzaldehyde and also exhibited two absorption maxima located at 345 and 287 nm. The absorption spectrum in acetonitrile solution is shown on figure 6.3.1.

22
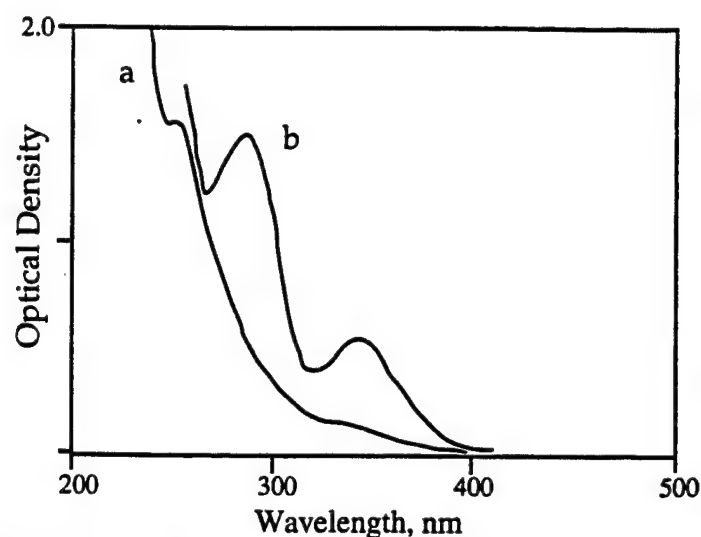
Fifure 6.3.1. Absorption spectra of nitro-benzaldehyde,a, and nitro-naphthaldehyde, b.

There is significant absorption at 355 nm which makes this material suitable for application in two-photon processes involving 1064 and 532 nm laser beams. The two-photon writing precess in nitro-naphthaldehyde based material is shown in scheme 1:

acid generator		acid

1064nm + 532nm

dye precursor   acid   colored dye, "Read" form
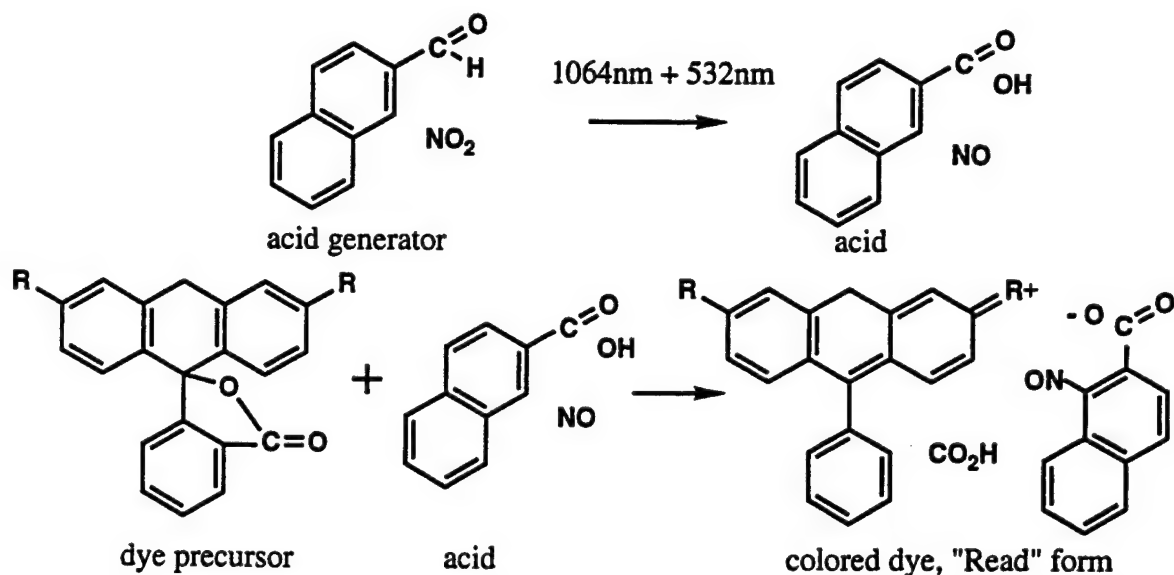
Scheme 1.

Light excitation of the material synthesized with $\lambda < 400$ nm induces a photoreaction which results in the formation of the product which has an absorption spectrum also shown in figure 6.3.1. Further analytical studies of this product reveal that this molecule is, as expected, acidic and is therefore capable of reacting with the dye precursor to produce the colored dye, Rhodamine B, which has a very high fluorescence efficiency. Our experiments show that the photochemical transformation of nitronaphthaldehyde has a relatively high efficiency of above 50%. The properties of this material suggest that it is the best material known so far, for utilization in storage and retrieval of 3D information.

The spectroscopic and kinetic properties of 2-nitro-naphthaldehyde in liquid and dispersed in different polymer matrices were studied in detail.

23

Our experiments show that this new acid generator has very high solubility in the monomers which were tried. It was also possible to make polymer cubes with a concentration of acid generator, about 40 mg/ml. These polymer concentrations are much higher than the previous acid generator materials and constitute a crucial parameter for practical 3D memory devices because they allow for high density unit area of written molecules.

However, acid generator concentrations of more than 40 mg/ml lead to a significant decrease in the rate of polymerization. This slow polymerization rate results in rather soft polymer blocks even after prolonged polymerization. The best quality of memory materials having very good optical quality were obtained with a concentration of ~30 mg/ml of acid generator.The experimental data suggests that the polymerization process may be responsible for the increase of the background fluorescence intensity emitted from the memory cubes. To understand how to minimize this fluorescence background radiation, we studied polymerization under various conditions.

It was found, that the best optical quality polymer cubes with low background color were prepared from methylmethacrylate monomer alone or with the addition of acrylonitrile monomer in a 3:1 ratio. Copolymerization with acrylonitrile monomer leads to an increase in the polymer polarity which increases the concentration of the "written" form of memory material. For high writing efficiency and low intensity of background fluorescence the optimum concentration of the precursor such as Rhodamine B was found to be 0.05 mg/ml.

Our experiments show, that the memory cubes with light sensitive acid generators concentrations of about 30 mg/ml were sensitive enough to write information inside the volume by a two-photon absorption. In these experiments the scattered background fluorescence intensity was much lower compared to the fluorescence intensity from the written bits.

The written form was found to be stable at room temperature, and no information was lost, stored as depicted by the experimental data which show that practically no change in written images intensity occurred while the written memory cube was stored in the dark for two months.

6.4. Thermal equilibrium in the dye precursor - dye system.

The reaction of coloration between acid and Rhodamine B Lactam was found to have a reversible nature and the written colored form, in principle, can be bleached back to the colorless Lactan form by adding appropriate amount of base. The chemical reaction between the acid and the Lactame form, which is responsible for writing process in the ROM material may be presented by the following scheme:
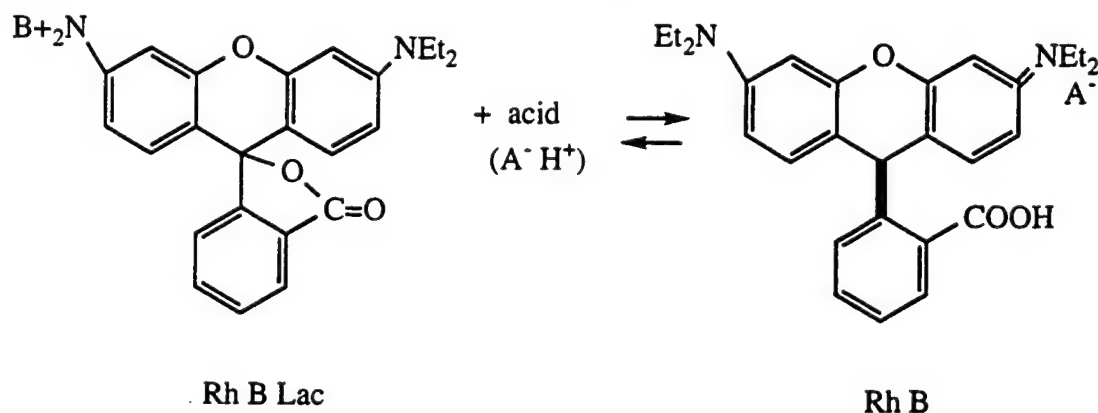
This reversible reaction equilibrium constant, K, is calculated from equation:

$$K = \frac{[Rh\ B]}{[Rh\ B\ Lac] \times [acid]},$$

where [Rh B], [Rh B Lac] and [acid] are equilibrium concentrations of written form dye precursor and acid correspondingly. The value of equilibrium constant K is a very important parameter because it characterizes the strength of acid, or, in other words, the ability of the generated acid to perform the molecular reaction which is a necessary precursor of the writing process. Our recent experiments show that different organic and inorganic acids have considerable difference in K value in reaction with Rh B Lac therefore they will influence the rate and efficiency of information input at significantly different levels. We have measured the K values for number of acids, including nitrosoacid, produced by photolysis of 2-nitro-naphthaldehyde. The measurements were conducted in dichloroethane solutions, which have a polarity value close to the one for PMMA, (PMMA is the host polymer used for preparation of memory cubes). Exact concentrations of dye precursor and acids, about 10^{-6} M, were prepared for these measurements. The equilibrium concentrations of the reagents were calculated from the absorption spectra of the solutions and K values were calculated for the various acids investigated. As was shown in the previous report, it is possible to convert 2-nitro-naphthaldehyde acid generator almost quantitatively to the corresponding nitroso acid. We used this property of 2-nitronaphthaldehyde for the preparation of the exact concentration of nitroso acid solutions required to calculate K values.

Table 6.4.1

Acid	K
Acetic acid	4
Benzoic acid	24
Nitroso-acid from NNA	308
HCl	15000

The values of the equilibrium constants K for the reaction of different acids with Rhodamine B Lactam are listed in table 6.4.1. As shown in table, the K value of nitroso acid produced by photolysis of 2-nitronaphthaldehyde is relatively high, compared to other organic acids. This increase in acidity strength could be due to the introduction of a polar -N=O nitroso group into the ortho-position of the molecule. The molecule, which does not have this polar group in its structure, such as benzoic acid, has considerably lower acidity. For nitrosoacid, which is the material used in ROM devices, the equilibrium constant, K, was found to be K = 300. This value means that reaction between 300 molecules of Rhodamine B Lactame and 300 molecules of nitrosoacid will produce ~ 299 molecules of the written form and leave only 1 molecule of each of the reagents. In other words, practically all molecules (99.7%) of dye precursor, or write form, will be transferred to the written form.

6.5. Transient absorption spectra and kinetics

We studied the detailed mechanism of the photochemical transformation of nitronaphthaldehyde leading to the corresponding nitroso-acid. This is the primary step of the writing process in our ROM material. The experiments show, that the excitation of nitronaphthaldehyde in solution with 355 nm ultrafast laser pulses results in the appearance of a fast intermediate with a long wavelength absorption band maximum at 580 nm. We studied the effect of different solvents on the absorption spectra and lifetimes of this intermediate. The various solutions of nitro-naphthaldehyde were irradiated with 25 picosecond and 6 nanosecond Nd-YAG lasers at 355 nm laser pulses. Our experimental data suggests that

25

polar solvents such as acetonitrile and alcohol stabilize the intermediate state and consequently increase its lifetime. The energy decay kinetics of this transient measured at the wavelength of maximum intensity of its absorption band, 580 nm, in different solvents. The lifetime of the transient decreases from 200 ns in iso-propanol to 100 ns in dichloroethane to 50 ns in benzene. We were not able to detect any transients with absorption above 450 nm, when nitroaldehyde was dissolved in nonpolar hydrocarbons, such as cyclohexane, hexane or methylpentane. During these measurements, only the final stable nitroso-acid, which has its absorption maximum at about 400 nm, was observed. We also found, that the efficiency of the photochemical transformation of nitro-naphthaldehyde to nitroso-acid is practically the same in polar and nonpolar solvents. To detect the transient in nonpolar solvents, we used an experimental system which is capable of 30 picosecond time resolution, and allows us to measure spectra and kinetics of fast intermediates with lifetimes as long as tens of nanoseconds. Time resolved absorption spectra show that the transient in cyclohexane is formed practically completely within the excitation pulse duration. Figure 6.5.1 shows the absorption spectra, measured at 500 ps after excitation, this also shows that the absorption spectra of the transient in nonpolar cyclohexane are blue shifted by ~30-40 nm compared to the spectra observed in polar solvents. The increase in lifetime of the transient and the shift of its absorption spectrum to the long wavelength region with increase in solvent polarity indicates that the transient has a large dipole, which can be stabilized by polar solvent molecules.
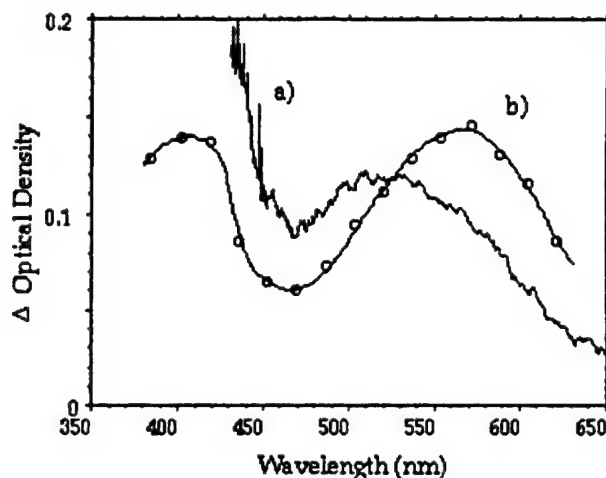

Figure 6.5.1. Transient absorption spectra of deaerated NNA solutions: a) in cyclohexane, 500 ps after excitation with 355 nm, 30 ps pulse; b) in acetonitrile after excitation with 355 nm, 6 ns pulse.

It is known, that in the case of benzaldehyde, which undergoes the same photochemical transformation as the naphthaldehyde used in ROM materials, an intermediate which has ketene structure was observed after the light excitation. This ketene intermediate is very sensitive to the presence of water. Consequently the decay lifetime is much faster if solvents contain water even in small concentrations. We studied the effect of water on the lifetime of the intermediate observed during photochemical reaction of nitro-naphthaldehyde. This is very important for devices because if complete absence of water is necessary then provisions must be made. As shown in our experiments, in the case of nitro-naphthaldehyde the presence of water in fact stabilizes the transient, rather than accelerating its decay as in the case of benzaldehyde. In a water-acetonitrile mixture the lifetime of the transient is about 300 ns, while in pure acetonitrile it is 1.5-2 times faster. This stabilization effect of water led us to suggest that in the case of nitro-naphthaldehyde the observed intermediate has a different structure than the ketene intermediate, formed by excitation of benzaldehyde.

To determine the nature of the observed transient we conducted several experiments on the influence of different substances, which may sensitize or quench the electronic excited states involved in the writing process. It was found that in the presence of oxygen, which is a very effective triplet excited state quencher, the decay rate of the transient is faster than in degassed solutions.
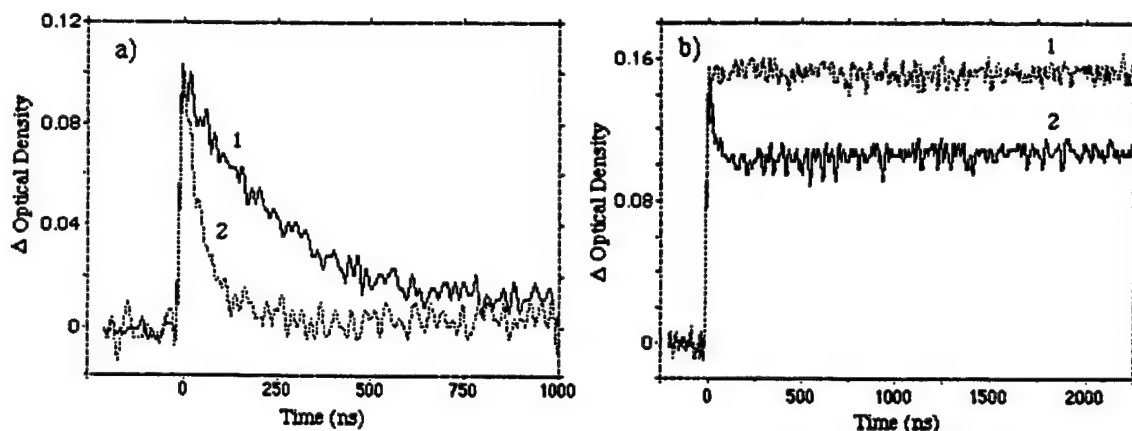

Figure 6.5.2. Effect of oxygen on transient kinetics in acetonitrile: a) measured at λ=570 nm in deaerated (1) and oxygen saturated (2) solutions; b) measured at λ=400 nm in deaerated (1) and oxygen saturated (2) solutions.

Figure 6.5.2 shows the kinetics of the nitro-naphthaldehyde transient in acetonitrile solutions saturated with oxygen and degassed under vacuum. In the presence of oxygen we observed acceleration of the transient decay rates when dissolved in polar solvents such as acetonitrile, alcohols, and dichloroethane. It is important to note, that while oxygen has a strong effect on the transient decay rate, the absorption intensity of the transient, measured at 0-time (the time right after light excitation) is not effected by the presence of oxygen. At the same time, we observed a decrease in the absorption intensity maximum of the final nitroso-acid in the presence of oxygen, measured at 400 nm. The data obtained suggest the following mechanism for the photochemical reaction of nitro-naphthaldehyde:

$$NNA \xrightarrow{h\nu} S_1 \longrightarrow T_1 \longrightarrow (I) \longrightarrow NA$$
$$\xrightarrow{+O_2} S_0$$
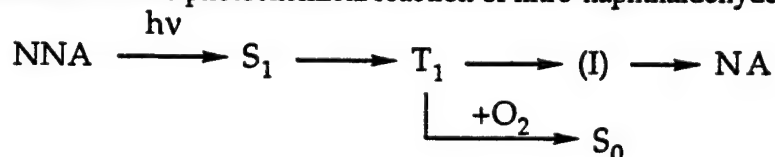
where S_1, T_1, and S_0 are the singlet excited state, triplet excited state, and ground state of nitro-naphthaldehyde respectively, I is the ketene intermediate, NA is stable nitroso-acid. Based on our experimental data, we assign with confidence the triplet excited state to the transient observed during the photolysis of nitro-naphthaldehyde.

To confirm the triplet nature of the photoactive electronic excited state, we conducted several experiments at low temperature, 77K. In these experiments the solution of nitronaphthaldehyde in EPA or iso-propanol was deaerated by sequences of freeze-thaw cycles carried out under vacuum conditions. The cell with investigated solution was placed in liquid nitrogen Dewar with optical windows. A 355 nm laser pulse was focused inside this cell with nitronaphthaldehyde, dispersed in solid frozen matrix of EPA or iso-propanol. The photoinduced emission from the sample was collected by system of lenses and focused on the slit of monochromator, coupled to PMT. The signal from PMT was monitored by digital oscilloscope connected to computer.

We found that excitation of nitronaphthaldehyde in solid matrix at 77K followed by strong phosphorescence, which is an indication of involvement of the triplet excited state in

27

this photochemical reaction. It was also found that photochemical transformation of nitronaphthaldehyde to nitrosoacid proceeds at low temperature, 77K, with the quantum efficiency an order of magnitude lower than at room temperature.

To measure the quantum efficiency at low temperature special solutions of nitronaphthaldehyde with exact volume and concentrations were prepared. The light excitation of these solutions with 355 nm laser pulses were conducted at room and 77K temperatures. The cell with solutions or frozen matrices was placed in the fixed place in experimental system, so that the number of absorbed photons by nitronaphthaldehyde molecules was the same for all measurements. The difference in concentrations of accumulated nitrosoacid was proportional to quantum efficiency of the photoprocess. The quantum efficiency values for photorearrangement of nitronaphthaldehyde to nitrosoacid at different temperatures were calculated from these data and listed in table 6.5.1.

Table 6.5.1. Quantum Efficiency for the Conversion of NNA to Nitrosoacid

Solvent	Temperature, K	Quantum Efficiency
EPA	295	0.50
EPA	77	0.01
3-Methylpentane	295	0.50
3-Methylpentane	77	0.04
Methylcyclohexane	295	0.51
Methylcyclohexane	77	0.04

It was found that phosphorescence spectrum of nitronaphthaldehyde dispersed in EPA matrix at 77K has its maximum at 550 nm, as shown in figure 6.5.3. The phosphorescence lifetime was calculated from the data, shown in figure 6.5.4, were the phosphorescence intensity plotted as a function of time. The phosphorescence lifetime of nitronaphthaldehyde in EPA at 77K was found to be 75 msec.

We also found that in non-polar matrix, such as methyl-pentane, at 77K phosphorescence intensity was lower than in polar EPA matrix, while the quantum efficiency for photoreaction was higher. The quantum efficiency data for phototransformation of nitronaphthaldehyde to nitrosoacid at different temperatures, presented in table 6.5.1, suggest that at 77K the deactivation of the triplet excited state occurs mainly by emission of phosphorescence photons rather than by photochemical reaction.
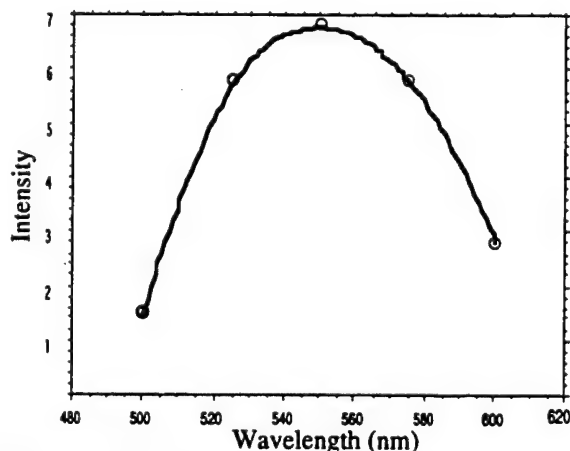
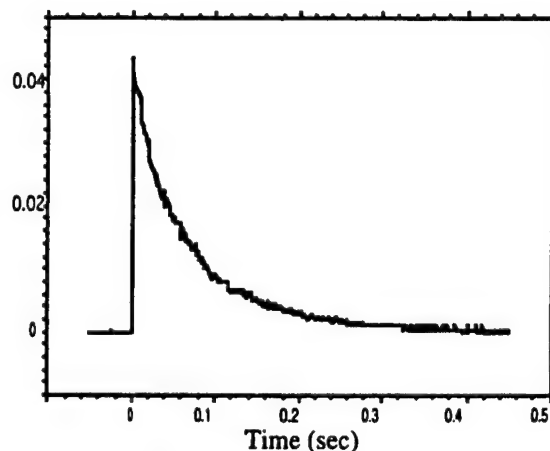Figure 6.5.3. Phosphorescence spectrum of NNA in EPA at 77K

Figure 6.5.4. Phosphorescence kinetics of NNA in EPA matrix at 77K

28

3D MEMORY SYSTEMS

1. Scope of the program and Summary of Results:

This program had two main objectives:
a) The development of a suitable technique to delay short optical pulses to enable the counter propagating pulse addressing (CPPA) architecture developed for fast access two-photon memory systems.
b) The investigation of different spatial light modulator technologies for their suitability for parallel recording by two-photon absorption.

We have reached both objectives successfully by first demonstrating the feasibility of an optical pulse delay device based on an acousto-optical modulator that is capable of 60 programmable delays capable of switching in about a microsecond. By cascading two such devices, it is possible to generate more than 1000 pulse delays and therefore accessing 1000 recorded planes in a two-photon memory device based on the CPPA architecture with access times in the order of a few microseconds. In addition, the demonstrated device can be useful in a variety of other applications including phase array antennas. The details of the design and experimental demonstration and characterization of this optical pulse delay device is provided in Section 2.

Second we have conducted a study of suitable Spatial Light Modulator (SLM) Technologies for performing parallel writes on two-photon memories. The technologies that we studied included PLZT light modulators, TI's deformable micro-mirror device, Liquid Crystal SLMs, and the possibility of using Multiple Quantum Well absorption modulators. Our studies revealed that PLZT modulators could handle the high peak optical power required to record by two-photon absorption by modulating 1064nm wavelength with about 10:1 contrast. The contrast was however, significantly lower for 532nm wavelength due to residual absorption of PLZT at this wavelength. The photo-generated carriers screen the applied effective field reducing effectively the electrooptic modulation.

We found that the TI devices were capable of handling the peak optical powers required, both at 532 and 1064 nm. The contrast was good (6:1). However, for unexplained reasons the devices failed to operate longer than a few hours under optical bias. The failure mechanism is presently unknown and a detailed study beyond the scope of this program would be required to determine the causes of this type of failure.

The Liquid Crystal devices that we studied were obtained from different sources including DisplayTech and Boulder Non-linear systems. They all did modulate at 532nm but the contrast ratio obtained at 1064 nm were very low (~2:1) and therefore not suitable for recording by two-photon absorption at this wavelength. However, optimized devices for this wavelength should perform better.

Finally, MQW absorption modulators did not perform well at the required optical intensities because of their saturation properties. However, we did observe a phase modulation at 1064 nm from these devices and the potential use of this type of modulation is being investigated in another more recently funded program.

In summary, in terms of performance TI devices performed best as long as they lasted. However, the failure mechanism must be investigated further. Therefore, we

30

recommend the use of either PLZT or Liquid Crystal devices for future experiments. However, the devices need to be optimized for contrast ratio for the desired wavelength.

2. Optical pulse delay for counter propagating pulse addressing

Counter propagating pulse addressing provides an alternative scheme to access data in a 3-D volume. Two optical beams carrying short pulses counter propagate within the same path. In locations where two pulses overlap temporally and spatially two-photon recording occurs. In order to reduce the intersection volume and to increase the longitudinal bit resolution, ultra short pulsed lasers must be used.

Addressing in the counterpropagating-pulse scheme can be accomplished by applying a delay to one of the pulses relative to the other as depicted in Figure 2-1. By varying the amount of the delay applied to each addressing pulse, we can select the intersection plane where the two pulses overlap along the propagating path, and achieve random bit addressing. The design configuration and preliminary demonstrations of an acousto-optical programmable phase delay device were developed during this program.
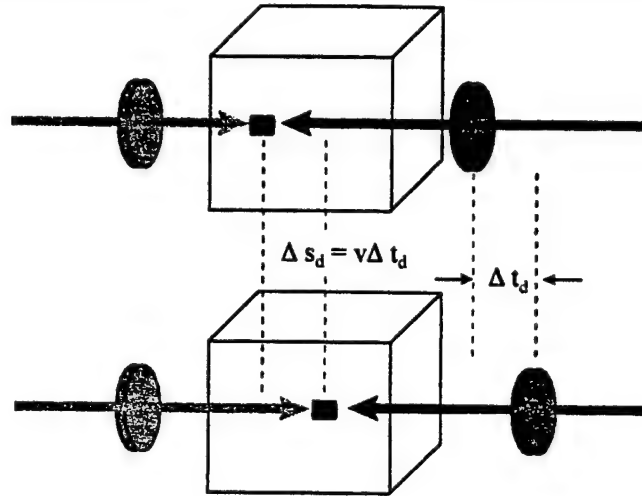

Figure 2-1   Illustration of addressing method in the counterpropagating-pulse scheme which is achieved by applying a delay to the addressing pulse.

In principle, the capacity of the two-photon storage devices based on counter propagating pulse addressing can be expressed as a function of the optical wavelengths λ_i and the spatial pulse width pw_i of the optical beams as

$$Capacity \propto \left(\frac{n_1 pw_1 + n_2 pw_2}{n_1 + n_2} \cdot \lambda_1^2 \right)^{-1},$$

provided that $\lambda_1 < \lambda_2$. The first term in the parenthesis determines the longitudinal dimension of the bit size with n_1 and n_2 representing the refractive indices of the material seen by the pulses at the two wavelengths. It should be noted that the longitudinal bit size is dependent on the duration of the optical pulses used in the addressing scheme.

31

The counter propagating pulse collision addressing becomes a powerful approach when used for accessing data in microchannel media. This media configuration consists of a large number of microchannels where the two-photon storage material is used as the core of each microchannels as shown in Figure 2-2. This media configuration may resemble the structure of a fiber bundle in which each channel takes on the form of a single-mode or multimode waveguide with appropriate claddings to permit waveguide functionality. Counterpropagating pulse addressing may be used with microchannel media as illustrated in Figure 2-3.
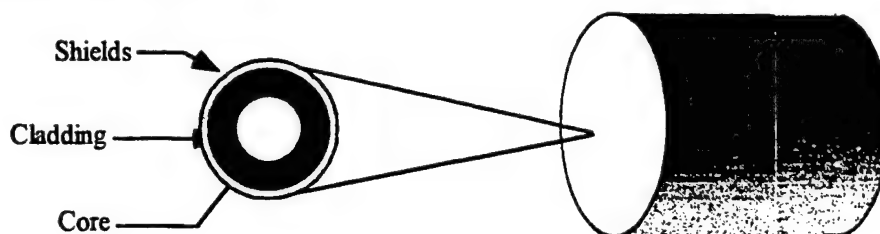

Figure 2-2   Conceptual structure of a microchannel memory device.
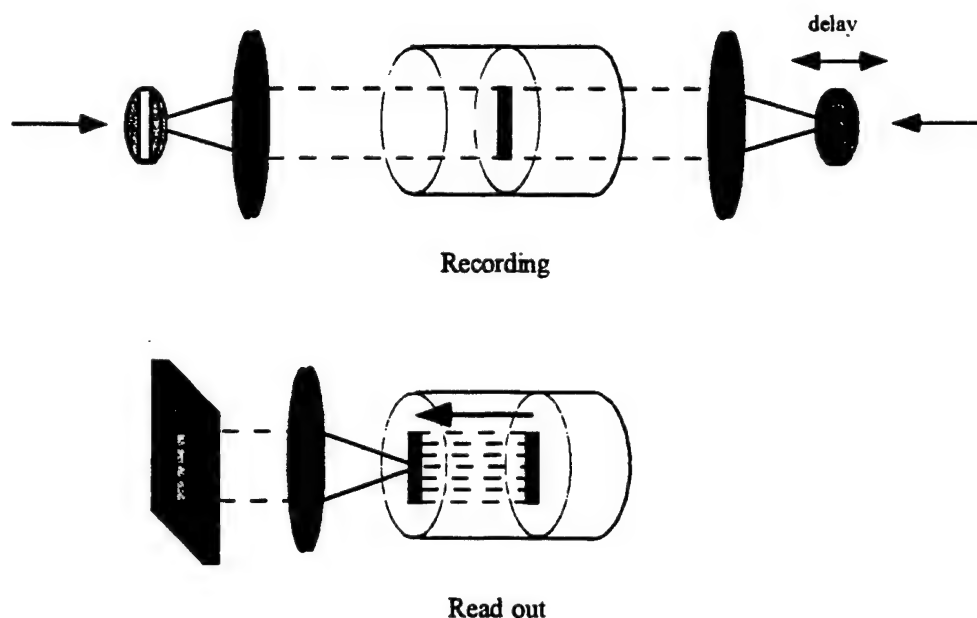

Recording

Read out

Figure 2-3   Operations of the two-photon microchannel memories based on counterpropagating pulse addressing.

Data is recorded into the microchannel memory imaging the information to be recorded onto the microchannel media surface. Each pixel of information is then guided in the microchannels. From the back surface of the microchannel media a second uniform beam is coupled into each micro channel. The information bits of interest are then recorded at the points of intersections of the optical pulses counter propagating in the microchannels. By delaying one puls with respect to another one can then access the entire volume of the microchannel media. Data retrieval is accomplished by again accessing the desired location by counter propagating infra red beams. The fluorescence

generated by two-photon absorption at recorded bits of interest is guided within the microchannel and detected at the output of each channel as depicted in Figure 2-4.
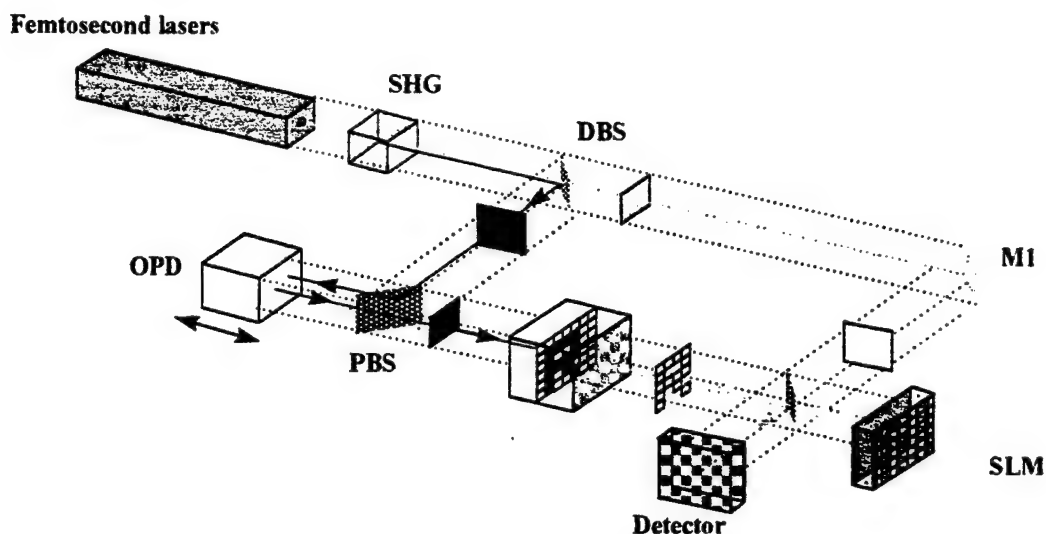

Figure 2-4   Possible configuration of the two-photon microchannel storage system. (SHG = Second Harmonic Generation, DBS = Dichroic Beam Splitter, SLM = Spatial Light Modulator, PBS = Polarizing Beam Splitter, and OPD = Optical Pulse Delay, M1 = Mirror)

Therefore counter propagation pulse collision addressing is an elegant method to access the volume of a microchannel media. However, for fast access of large number of bits a fast programmable phase delay element must be made available. During this program we developed such a suitable Optical Phase Delay OPD device.

The capacity of such a memory device is dependent on the duration of the optical pulses. In order to maximize the device capacity, ultrafast pulses in the femtosecond regime should be used. However, ultra fast pulses are susceptible to dispersion effects which consequently broaden the pulse width. Thus, the OPD device must be dispersion-compensated to maintain a small pulse width. In addition the device must be capable of resolving at least 1000 phase delays and be able to switch between these programmed delays within a microsecond.

Principles of operation of the OPD

Our approach uses an acousto-optic deflector (AOD) to send the input beam along various paths. Each path has a distinct and precise length which is controlled by a stepped mirror. The principal elements in our design of the Optical Pulse Delay (OPD) device are an acousto-optic deflector and a stepped mirror as illustrated in Figure 2-5.
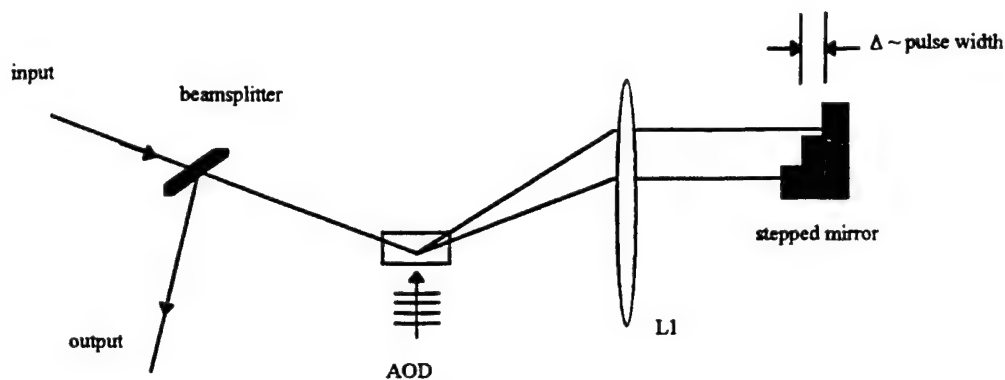
Figure 2-5:Diagram showing the principles of operation of the OPD system.

The acoustooptic deflector (AOD) deflects the optical beam into the first diffraction order with a deflection angle determined by $\theta = \sin^{-1}(\lambda f/2nv)$, where λ, f, v, and n are the optical wavelength, the acoustic frequency, the acoustic velocity, and the material index of refraction, respectively. Lens $L1$ is located one focal length after the AOD and redirects the beam to normally incident onto the stepped mirror. The stepped mirror provides the required path lengths to delay the optical pulses. The input and output beams are then separated from each other by a beamsplitter.

This design can be improved in terms of power efficiency by replacing the beamsplitter with a combination of a polarizing beamsplitter and a quarter wave plate such that the input and output beams can have orthogonal polarizations and will be separated completely with the polarizing beamsplitter. An alternative method to improve power efficiency is to choose an anisotropic material as the A-O cell. It has been found that when the anisotropic A-O cell is operated in a shear mode, i.e. the displacement of the dipoles is perpendicular to the direction of the acoustic wave, the polarization of the optical beam can be changed after diffraction through the cell.[8] Hence, by carefully choosing the A-O cell such that the polarization of the input beam will be rotated by 45 degree after each diffraction, we can arrange the input and output beams to have orthogonal polarizations. This approach eliminates the need for the quarter wave plate and renders the system less dispersive.

An ultrafast optical pulse is composed of a spectrum of monochromatic waves having a precise phase relative to each other. According to Fourier analysis, the time duration and the frequency spectrum of any pulses are related by $\Delta\tau\Delta f \; ? \; \frac{1}{4\pi}$.[9] Thus, the shrinking of the frequency spectrum would enlarge the temporal duration of the pulses. Therefore, an important parameter in the design of this OPD system is chromatic dispersion. This effect can cause beam smearing, which in turn results in the reduction of the time-bandwidth product of the AOD and pulse distortion. The latter is a result of a spatial separation of the frequency spectrum of the input beam. If the diffracted beam from the AOD was taken as the output without any correction, it would distort the shape of the output pulse since each frequency component is no longer in phase with one another. Further, some of the components may be missing if only part of the beam is taken as the output.

Since the capacity of the microchannel memory based on counterpropagating pulse addressing is determined by the pulse width, any distortion or broadening of the pulse is

undesirable. The double-pass geometry shown in Figure 2-5 elliminates this problem. The basic idea is that any physical separation of the pulse spectrum caused by the AOD will be undone by the second pass through the A-O cell in the reverse direction. Therefore, every spectral components will be recollected at the A-O cell and returned to its original form. We have shown experimentally that such a design can correct for this pulse broadening to within our measurement accuracy.

Design options

Although the system can be optimized in terms of power efficiency by using polarization effects, there are a few dispersive components involved in the design which may result in pulse broadening. In order to make the system less dispersive, the lens can be replaced with a parabolic mirror. We also introduce a skew geometry to separate the input and output beams without using polarization effects. In this case, our final approach is conceptually arranged as shown in Figure 2-6.
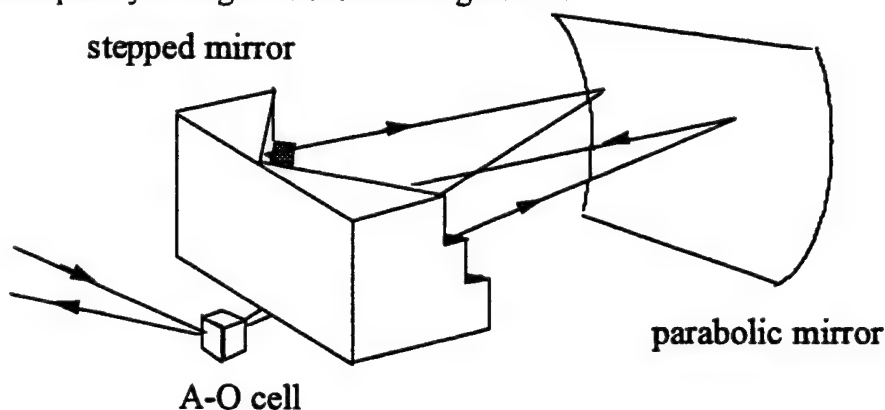

Figure 2-6 Schematic diagram of the improved OPD system.

The system in Figure 2-6 has the same functionality as the one before, except that it provides better performance in terms of power efficiency and pulse dispersion by completely eliminating the polarizing beamsplitter and the lens, respectively. It also removes the constraint of requiring anisotropic A-O cell material and hence provides more flexibility to choose the components for the system. By replacing the lens with a reflective parabolic mirror, the system becomes less dispersive. In addition, the stepped mirror, rather than having a rectangular-staircase shape, is constructed in a V-shaped configuration in order to introduce symmetry and accommodate the off-axis beams. The input and output beams are separated as a result of the skew geometry. Optical pulses arriving at the Bragg angle onto the acousto-optic deflector will be deflected off and redirected to the stepped mirror by the parabolic mirror. The required delay or path length which is provided by the stepped mirror is thus selected by the acoustic frequency. The beam is returned to the parabolic mirror and back to the acousto-optic deflector. Due to the system symmetry, the returning beam will arrive at the Bragg angle and will be diffracted at a slight angle from the original incoming beam, resulting in a spatially separated input and output beams.

The performance of the OPD is mostly determined by the effectiveness of the acousto-optic deflector. For example, the number of planes or delays that the OPD can provide, will be governed by the time-bandwidth product of the AOD. The speed of

35

operation of the OPD is determined by the access time of the AOD. In addition, the cascadability of the OPD is ultimately determined by the diffraction efficiency of the AOD. Finally, the only dispersive component in this approach is the A-O cell, and thus pulse broadening, if any, will be a direct consequence of the material dispersion of the acousto-optic material.

Experimental setup and results

The purpose of the experiment was to demonstrate that ultrafast pulses can be successfully delayed with the proposed optical pulse delay component. This can be accomplished with the knowledge that when two laser beams are spatially and temporally coherent, their interference fringes can be observed. Since pulsed lasers have a coherence length that is at most as large as its pulse width, we have used an interferometeric technique to identify the presence of pulse overlap. For example, a 100-fs pulse has a corresponding spatial width of 30 μm. The spatial correlation width between two 100-fs pulses is thus 60 μm. If two pulses are present at the same time and are less than 30 μm apart in space, interference fringes should be observed. Clearly, if one pulse is delayed with respect to the other, they will no longer overlap in time and fringes will disappear.

In the experiment, the OPD system was placed in one arm of a Michelson interferometer. The second arm was used as a reference. Since the coherence length of the laser is on the order of its pulse width, the reference mirror must be moved such that the path length on both arms are matched and fringes are visible at the output. The schematic diagram of the setup is depicted in Figure 2-7. An Ar^+-pumped Ti:Sapphire laser operating at 960 nm was used to produce 130-fs mode-locked pulses. This laser has a repetition rate of 76 MHz. Each pulse had a spatial width of approximately 40 μm and was separated from one another by approximately 4 meters. A 50:50 beamsplitter was used to split the optical beam into two orthogonal arms. In the arm consisting of the OPD design, a TeO_2 AOD with a center frequency at 80 MHz and a bandwidth of approximately 40 MHz was used. The stepped mirror was made from microscope slides which were stacked and then glued together. To make it reflective, we evaporated a 1 μm gold layer on to the surface. Each step was approximately 1 mm apart.
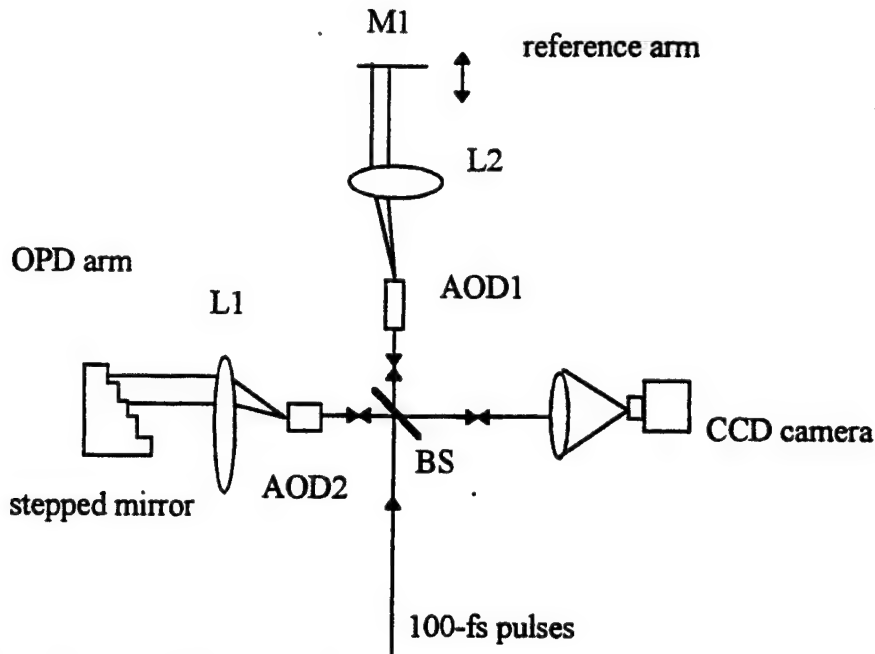
Figure 2-7Michelson interferometer setup for the OPD experiment; M1= mirror, L = lens, AOD = acousto-optic deflector.)

In the reference arm, the second AOD was used to correct for the frequency shift of the laser beam such that the interference fringes would be stable. This, however, is not required in the operation of the OPD which is not based on interferometry. The delay in this arm was controlled by a flat translating mirror which was located at the end of the arm. Both AODs were driven by an analog RF amplifier. The RF signal was generated by a Fluke 6060B signal generator which allows a direct-random frequency input or a continuous frequency sweep. The lenses were located one focal length away from the acousto-optic cells and refracted the beams to travel parallel to the optic axis and perpendicular to the mirror surface. In the output arm, a 6x microscope objective was used to expand the beams. Fringe images were then captured on a Photometrics CCD camera.

The experiment was performed at three distinct delays provided by the stepped mirror. Each delay was achieved by setting the acoustic frequency such that the optical beam was directed to the desired step. In this experiment, the frequencies were 54, 82 and 106 MHz which correspond to three adjacent steps on the stepped mirror. The location of the flat mirror in the reference arm was adjusted to match the path length of the optical pulse delayís arm. Once fringes were detected, their location was marked as A, B, and C, respectively, for each frequency.

Figure 2-8 shows the images captured by the CCD camera at different combinations of the acoustic frequency and the flat mirror position. At 54 MHz, fringes were present at position A while no fringe was observed at position B and C. For 82 MHz, fringes were observed at position B while they were absent at position A and C. And at 106 MHz, fringes were seen only at position C. For each given acoustic frequency, the fringes can only be observed at only one of the mirror location. The optical path lengths in the two

37

arms, are within the spatial correlation width of the two pulses (< 60 μm). This demonstrates that we have successfully delayed femtosecond pulses using the acousto-optic deflector and the stepped mirror configuration.
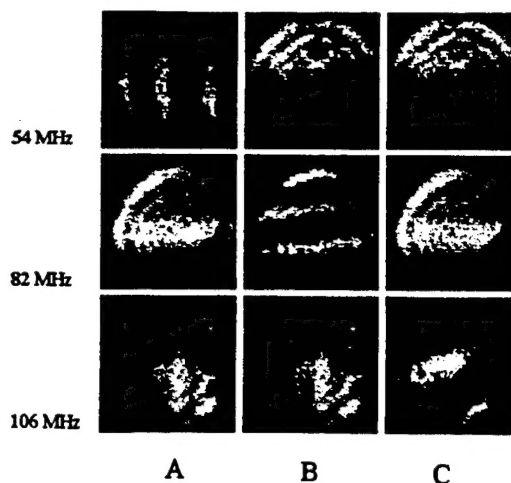

54 MHz

82 MHz

106 MHz

A   B   C

Figure 2-8   Fringe images as seen at various flat mirror locations at each acoustic frequency.

System limitations due to ultrafast optical pulses considerations

The time domain and the frequency domain expression of ultrafast pulses are related by the Heisenberg uncertainty principle, $\Delta E \Delta t$? $\hbar$.[10] That is, for any pulses to have a short temporal duration (Δt), its associated frequency spectrum (Δv) must be large. This can also be viewed as a direct consequence of Fourier analysis, i.e. a short pulse is a coherent superposition of many individual sinusoidal frequencies whose amplitudes add constructively at one point in time. In most situations AODs are used with CW lasers which can be considered quasi-monochromatic light sources. However, when the incident light can not be considered quasi-monochromatic, other factors must be taken into considerations. For example, ultrafast pulses which possess a significant frequency spectrum, when being diffracted from the AOD will have a color spreading in the emerging beams. Such an effect tends to cause beam smearing and may result in a reduction of the time-bandwidth product, or the number of resolvablespots. Other effects including the reduction in the diffraction efficiency are also observed. We have studied and characterized these effects in greater detail as described in a paper published in Applied Optics that resulted from this program (Paper 3). Our studies included effects on
  - Diffraction efficiency
  - Color spreading and
  - Impact of Dispersion of materials

Our analysis indicate that an OPD with the required characteristics for CPPA architectures can be made readily available with the scheme developed during this program.

38

3. Publications that resulted from this program

1) J. Ford, S. Hunter, R. Piyaket, S. Fainman, S. C. Esener, S. Dvornikov, and P. Rentzepis, "3-D two photon memory materials and systems," *Proc. SPIE, OE Laser 93, Los Angeles* V1853, pp. 5-13, March 1993.

2) R. Piyaket, I. Çokgör, S. C. Esener "Three-dimensional memory system based on two-photon absorption," presented at *SPIE '94, Very Large Optical Memories: Materials and System Architectures Conference* 2297, San Diego, (12 pages), 24-29 July 1994.

3) Ram Piyaket, Susan Hunter, Joseph E. Ford, Sadik Esener, "Programmable ultrashort optical pulse delay using an acousto-optic deflector," *Applied Optics,* 34 (8), pp. 1445-1453, March 1995.

4) Ram Piyaket, Ilkan Cokgor, Frederick B. McCormick, Sadik Esener, Alexander S. Dvornikov, Peter M. Rentzepis, "Two-photon absorption based optical recording in organic planar waveguide," *OSA Annual Meeting & Exhibit, 11th Interdisciplinary Laser Science Conference, Portland, OR,* (Submitted to Optics Letters), September 1995.

References

1. R. R. Hayes, and D. Yap, iGaAs spiral optical waveguides for delay-line applications,î Journal of Lightwave Technology **11**, pp. 523-527 (1993).

2. G. Barbarossa, and P. J. R. Laybourn, iNovel architecture for optical guided-wave recirculating delay lines,î in *Advances in Optical Information Processing V*, D. R. Pape ed. (SPIE, Bellingham, Washington, 1992), pp. 138-144.

3. P. Morin, D. Chiaroni, and J. B. Jacob, iPhotonic time-switching using semiconductor optical amplifier gates and fibre delay line optical buffer,î in *Photonic Switching*, A. M. Goncharenko, ed. (Andrei Marchovich, 1992), pp. 476-479.

4. D. Dolfi, F. Michel-Gabriel, S. Bann, and J. P. Huignard, iTwo-dimensional optical architecture for time-delay beam forming in a phased array antenna,î Optics Letters **16**, pp. 255-257 (1991).

5. N. A. Riza, iTransmit/receive time-delay beam-forming optical architecture for phased-array antennas,î Applied Optics **30**, pp. 4594-4596 (1991).

6. D. C. Edelstein, R. B. Romney, and M. Scheuermann, iRapid programmable 300 ps optical delay scanner and signal-averaging system for ultrafast measurements,î Review Scientific Instruments **62**, pp. 579-582 (1991).

7. K. F. Kwong, D. Yankelevich, K. C. Chu, J. P. Heritage, and A. Dienes, ì400-Hz mechanical scanning optical delay line,î Optics Letters **18**, pp. 558-560 (1993).

8. R. W. Dixon, ìAcoustic diffraction of light in anisotropic media,î IEEE Journal of Quantum Electronics **QE-3**, pp. 85-93 (1967).

9. J. Petykiewicz, *Wave optics*, (Kluwer, Dordrecht, The Netherlands, 1992).

10. A. Yariv, and P. Yeh, *Optical waves in crystals*, (Wiley-Interscience, New York, 1984).

11. E. I. Gordon, ìA review of acoustooptical deflection and modulation devices,î Proceedings IEEE **54**, pp. 1391-1400 (1966).

12. ìAll about Bragg angle errors in acousto-optic modulators and deflectors,î Isomet application note (Isomet Corporation, Springfield, Virginia 22151, 1977).

13. C. Huang, M. T. Asaki, S. Backus, M. M. Murnane, and H. C. Kapteyn, ì17-ps pulses from a self-mode-locked Ti:sapphire laser,î Optics Letters **17**, pp. 1289-1291 (1992).

14. V. V. Petrov, ìHigh frequency (up to 10 GHz) acoustooptics-the way of development,î SPIE **1844**, pp. 342-349 (1992).

15. R. L. Fork, O. E. Martinez, and J. P. Gordon, "Negative dispersion using pairs of prisms," Optics Letters **9**, pp. 150-152 (1984).

MISSION
OF
AFRL/INFORMATION DIRECTORATE (IF)

The advancement and application of information systems science and technology for aerospace command and control and its transition to air, space, and ground systems to meet customer needs in the areas of Global Awareness, Dynamic Planning and Execution, and Global Information Exchange is the focus of this AFRL organization. The directorate's areas of investigation include a broad spectrum of information and fusion, communication, collaborative environment and modeling and simulation, defensive information warfare, and intelligent information systems technologies.